Probabilistic load flow in systems with high wind power penetration.

Julio Usaola
Departamento de Ingeniería Eléctrica
Universidad Carlos III de Madrid
e-mail: jusaola@ing.uc3m.es

Last review: August 22, 2008

Contents

1 Introduction.

The great proliferation of intermittent generation in power networks has increased the uncertainty in power systems. This uncertainty affects both the long and medium term system planning, and the day-ahead operation.

Probabilistic power flow is one of the best known probabilistic tools. From the first proposals in the seventies ([1], [2]), a great deal of literature can be found about this subject. The most straightforward method of solving this problem is Monte Carlo simulation. This technique involves repeated simulation with values obtained from the Probability Density Function (PDF) of the random variable considered. But for an adequate representation, many simulations must be considered in real systems. This makes this approach unpractical. One of the alternatives is the convolution of the PDF of the random variables involved, when they are independent of each other, and linearly related. Although this reduces the computational burden, it is still costly to obtain the PDF of a single line when several random power injections are considered. Fast Fourier Transform (FFT) techniques were proposed to reduce the computational burden [3], but this method is linked to the convolution technique, and does not solve the problem efficiently. In the early references, it was the uncertainty of the load what was considered. Reference [5] proposed the use of FFT and convolution in distribution networks, and makes a simplified estimation of the PDF for short term wind power prediction. A recent proposal is the Point Estimate method [4], that approximates the moments of the system variables of interest.

All these approaches assume that the random variables considered are independent. However, dependence between the uncertainties of power injection should be considered for loads and for wind generation. The generalization of some of these methods for considering the dependence between random variables is very complex, or unfeasible. There are some proposals that consider this dependence, only between loads, in [7], where it is modeled with a linear relation, and in [8], where the covariance has been taken into account in the equations.

Probabilistic load flow has mostly included the uncertainty of load. This uncertainty is not usually very high, especially for day-ahead operation, and it can be modeled using Gaussian probabilistic density functions. Wind energy proliferation, however, poses new challenges, since the variability of wind power production is much higher, usually the PDF are not Gaussian, and inputs are strongly correlated. Long term planning studies must consider PDF based on Weibull distributions, while short term operation analysis need to use PDF whose estimation is still under study.

The use of cumulants and the approximation of a PDF by orthogonal series (Gram Charlier A expansion series) have also been recently proposed [22]. It has interesting properties, and is computationally inexpensive. For large transmission networks it seems that this approach is very adequate due to the low computational requirements. It has the disadvantage of the necessary linearization but it may be easily generalized for dependent random variables. However, for non-Gaussian PDF, Gram Charlier A expansion series have serious convergence problems, and other approaches, such as Cornish Fisher expansion, give better results, without more computational burden [6].

The aim of this paper is to propose an analytical method (that will be called *Enhanced Linear Method* (ELM)) for the problem of probabilistic load flow. This method can be applied to grids where the wind power uncertainty, load uncertainty and generation availability must be considered. Mathematically, this means that the considered random variables may be continuous and/or discrete, and also dependent and/or independent.

The report is estructured as follows. First, the statistical theoretical background is given, with all the necessary definitions and concepts for the subsequent sections. Then, a short description of short term wind power prediction and its associated uncertainty follows. The load flow equations are written in order to give the nomenclature of the used variables and the conditions for their linearization. Afterwards, the probabilistic power flow methods examined are described, first the point estimate method, and its limitations, are given, with the necessary computational implementation. Then, the ELM approach is described under different assumptions, from simple conditions (independent continuous random variables) to a more general case (dependent continuous and discrete random variables). The study cases follow, with results commented and explained. A conclusion ends the report, with the main points of the study. Some appendices are given with additional information.

2 Statistics.

2.1 Basic concepts.

In this section, the basic concepts of Statistics are defined for an easier reading hereafter. The definitions follows [9]

Random Variable A random variable is a number $x(\zeta)$ assigned at every outcome ζ of an experiment. The resulting function must satisfy the following two conditions but is otherwise arbitrary.

1. The set $\{x \leq x_o\}$ is an event for every x.
2. The probability of the events $\{x = \infty\}$ and $\{x = -\infty\}$ equals zero.

Probability distribution function The probability cumulative distribution function (CDF) of the random variable x is defined as:

$$F(x_o) = P(x \leq x_o) \tag{1}$$

The properties of probability distribution functions are:

1. $F(+\infty) = 1$, $F(-\infty) = 0$
2. It is a non-decreasing function, if $x_1 < x_2$, then $F(x_1) < F(x_2)$
3. If $F(x_o) = 0$, then $F(x) = 0$, $\forall x \leq x_o$
4. $P(x > x) = 1 - F(x)$
5. $F(x)$ is continuous in the right, $F(x^+) = F(x)$
6. $P(x_1 < x < x_2) = F(x_2) - F(x_1)$
7. $P(x = x_0) = F(x_0) - F(x_0^-)$
8. $P(x_1 \leq x \leq x_2) = F(x_2) - F(x_1^-)$

Probability density function The probability density function (PDF), $f(x)$ is defined as:

$$f(x) = \frac{dF(x)}{dx} \tag{2}$$

2.2 Moments, cumulants and characteristic functions.

Moments Moments of order n are defined as:

$$m_n = E[x^n] = \int_{-\infty}^{\infty} x^n f(x) dx \tag{3}$$

$m_1 = \eta$ is the mean.

Central moments Central moments, or moments about the mean are defined as:

$$\mu_n = E[(x - \eta)^n] = \int_{-\infty}^{\infty} (x - \eta)^n f(x) dx \tag{4}$$

$\mu_2 = \sigma^2$ is the variance.

It can be demonstrated that:

$$\mu_n = \sum_{k=0}^{n} \left(\begin{array}{c} n \\ k \end{array} \right) m_k (-m_1)^{(n-k)} \tag{5}$$

$$m_n = \sum_{k=0}^{n} \left(\begin{array}{c} n \\ k \end{array} \right) \mu_k m_1^{(n-k)} \tag{6}$$

where

$$\left(\begin{array}{c} r \\ j \end{array} \right) = \frac{r!}{j!(r-j)!}$$

Characteristic function The characteristic function $\phi(\omega)$ associated to a random variable is defined as:

$$\phi(\omega) = E[e^{j\omega x}] = \int_{-\infty}^{\infty} f(x) e^{j\omega x} dx \tag{7}$$

There is an inversion formula, that gives $f(x)$ as a function of $\phi(\omega)$

$$f(x) = \frac{1}{2\pi} \int_{-\infty}^{\infty} \phi(\omega) e^{-j\omega x} d\omega \tag{8}$$

the similarity between these formulas and the Fourier transform must be remarked. The definitions of the Fourier transform and the inverse Fourier transform follow.

$$\begin{aligned} X(w) &= \int_{-\infty}^{\infty} x(t) e^{-j\omega t} dt \\ x(t) &= \frac{1}{2\pi} \int_{-\infty}^{\infty} X(\omega) e^{j\omega t} d\omega \end{aligned}$$

Moment generating function The moment generating function is similar to the characteristic function. It is defined as:

$$\phi(s) = E[e^s] = \int_{-\infty}^{\infty} f(x) e^{sx} dx \tag{9}$$

The following expression is called the **Moment Theorem**, and it says that

$$\phi^{(n)}(s) = \frac{d^n \phi(s)}{ds^n} = E[x^n e^{sx}]$$

and, therefore,

$$\phi^{(n)}(0) = E[x^n] = m_n \tag{10}$$

Hence, $\phi(s)$ could be expanded in its Taylor series

$$\phi(s) = \sum_{n=0}^{\infty} \frac{1}{n!} \phi^{(n)}(0) s^n = \sum_{n=0}^{\infty} \frac{m_n}{n!} s^n \tag{11}$$

This series converges only if the moments are finite, and in a close environment of $s = 0$.

Second characteristic function The second characteristic function, $\psi(\omega)$, is defined as:

$$\psi(\omega) = \ln \phi(\omega) \tag{12}$$

and, inversely,

$$\phi(\omega) = e^{\psi(\omega)}$$

Cumulants Cumulants of order n, κ_n are defined as

$$\frac{d^n\psi(0)}{ds^n} = \kappa_n \tag{13}$$

and it can be also written that

$$\psi(s) = \sum_{n=0}^{\infty} \frac{\kappa_n}{n!} s^n \tag{14}$$

From the expansion of both characteristic functions, it can be written that

$$\sum_{n=0}^{\infty} \frac{m_n}{n!} s^n = \exp\left\{ \sum_{r=1}^{\infty} \frac{\kappa_r}{r!} s^r \right\}$$

If the exponential is expanded in its Taylor series, and the terms of powers of s are equalled, the relations between moments and cumulants can be found. These expressions are better expressed in the recurrent formula (15).

$$\kappa_{r+1} = m_{r+1} - \sum_{j=1}^{r} \binom{r}{j} m_j \kappa_{r-j+1} \tag{15}$$

and $\kappa_1 = m_1$

The inverse formula for the central moments may also be written as (16).

$$\mu_{r+1} = \kappa_{r+1} + \sum_{j=1}^{r} \binom{r}{j} m_j \kappa_{r-j+1} \tag{16}$$

In the Appendix A, these relations are developed for the first terms.

2.3 Several random variables.

Let consider $\mathbf{x} = (x_1, \ldots, x_n)$ the vectorial variable formed from n scalar variables. In the following sections we will make $n = 2$ for simplicity's sake.

2.3.1 Distribution and density functions.

Joint distribution function The joint bivariate distribution function $F(x, y)$ is defined as

$$F(x_{1o}, x_{2o}) = P(x_1 \leq x_{1o}, x_2 \leq x_{2o}) \tag{17}$$

The properties of this joint distribution function are:

1. $F(-\infty, x_2) = 0$, $F(x_1, -\infty) = 0$, $F(\infty, \infty) = 1$
2. It holds that

$$\begin{aligned} P\{x_{1a} \leq x_1 \leq x_{1b}, x_2 \leq x_{2o}\} &= F(x_{1b}, x_{2o}) - F(x_{1a}, x_{2o}) \\ P\{x_1 \leq x_{1o}, x_{2a} \leq x_2 \leq x_{2b}\} &= F(x_{1o}, x_{2b}) - F(x_{1o}, x_{2a}) \end{aligned}$$

3. It also holds that

$$P\{x_{1a} \leq x_1 \leq x_{1b}, x_{2a} \leq x_2 \leq x_{2b}\} = F(x_{1b}, x_{2b}) - F(x_{1a}, x_{2b}) - F(x_{1b}, x_{2a}) + F(x_{1a}, x_{2a})$$

Joint density The joint density of x_1 and x_2 is by definition the function:

$$f(x_1, x_2) = \frac{\partial^2 F(x_1, x_2)}{\partial x_1 \partial x_2}$$

From this and property 1 follows that

$$F(x_1, x_2) = \int_{-\infty}^{x_1} \int_{-\infty}^{x_2} f(\alpha, \beta) d\alpha d\beta$$

Joint statistics It can be demonstrated that

$$P\{(x_1, x_2) \in D\} = \int_D \int f(x_1, x_2) dx_1 dx_2$$

where $\{(x_1, x_2) \in D\}$ is the event consiting of all outcomes ζ such that the point $[x_1(\zeta), x_2(\zeta)]$ is in D.

Marginal statistics In the study of several random variables, the statistics of each are called *marginal*. Thus $F_{x_1}(x_1)$ is the *marginal distribution* and $f_{x_1}(x_1)$ is the *marginal density* of x_1. It holds that

$$\begin{array}{cc} F_{x_1}(x_1) = F(x_1, \infty) & F_{x_2}(x_2) = F(\infty, x_2) \\ f_{x_1}(x_1) = \int_{-\infty}^{\infty} f(x_1, x_2) dx_2 & f_{x_2}(x_2) = \int_{-\infty}^{\infty} f(x_1, x_2) dx_1 \end{array}$$

Independence Two random variables x_1 and x_2 are called (*statistically*) *independent* if the events $[x_1 \in A]$ and $[x_2 \in B]$ are independent, that is, if

$$P\{x_1 \in A, x_2 \in B\} = P\{x_1 \in A\} P\{x_2 \in B\}$$

where A and B are two arbitrary sets on the x_1 and x_2 axes, respectively. If the random variables x_1 and x_2 are independent, then

$$F(x_1, x_2) = F_{x_1}(x_1) F_{x_2}(x_2)$$

hence

$$f(x_1, x_2) = f_{x_1}(x_1) f_{x_2}(x_2)$$

2.3.2 Joint moments

The *joint moment* of order $k + r = n$ of the random variables x_1 and x_2 is

$$m_{kr} = E\left[x_1^k x_2^r\right] = \int \int_{-\infty}^{\infty} x_1^k x_2^r f_{x_1 x_2}(x_1, x_2) dx_1 dx_2 \tag{18}$$

Thus $m_{10} = \eta_1$, $m_{01} = \eta_2$ are the first order moments, and the second order moments are

$$m_{20} = E[x_1^2] \quad m_{11} = E[x_1 x_2] \quad m_{02} = E[x_2^2]$$

The joint central moments of x_1 and x_2 are the moments of $x_1 - \eta_1$ and $x_2 - \eta_2$

$$\mu_{kr} = E\left[(x_1 - \eta_1)^k (x_2 - \eta_2)^r\right] = \int \int_{-\infty}^{\infty} (x_1 - \eta_1)^k (x_2 - \eta_2)^r f_{x_1 x_2}(x_1, x_2) dx_1 dx_2 \tag{19}$$

Clearly $\mu_{10} = \mu_{01} = 0$ and

$$\mu_{20} = \sigma_{x_1}^2 \quad \mu_{11} = C_{x_1 x_2} \quad \mu_{02} = \sigma_{x_2}^2$$

The *covariance* C or $C_{x_1x_2}$ of two random variables x_1 and x_2 is by definition the number:

$$C_{x_1x_2} = E[(x_1 - \eta_1)(x_2 - \eta_2)] = E[x_1x_2] - E[x_1]E[x_2] \tag{20}$$

where $E[x_1] = \eta_1$ and $E[x_2] = \eta_2$
The *correlation coefficient* ρ or $\rho_{x_1x_2}$ of the random variables x_1 and x_2 is by definition the ratio

$$\rho_{x_1x_2} = \frac{C_{x_1x_2}}{\sigma_{x_1}\sigma_{x_2}} \tag{21}$$

we maintain that $|\rho_{x_1x_2}| \leq 1$ and $|C_{x_1x_2}| \leq \sigma_{x_1}\sigma_{x_2}$
Two random variables are called *uncorrelated* if their covariance is 0. this can be expressed as

$$C_{xy} = 0 \quad \rho_{xy} = 0 \quad E[x_1x_2] = E[x_1]E[x_2]$$

Two random variables x_1 and x_2 are called *orthogonal*, notated as $x_1 \perp x_2$, if

$$E[x_1x_2] = 0$$

2.3.3 Characteristic function of joint random variables

The *joint characteristic function* of the random variables x_1 and x_2 is defined as:

$$\phi(\omega_1, \omega_2) = \int_{-\infty}^{\infty}\int_{-\infty}^{\infty} f(x_1, x_2)e^{j(\omega_1x_1+\omega_2x_2)}dx_1dx_2 \tag{22}$$

From this definition, it can be followed that

$$f(x_1, x_2) = \frac{1}{4\pi^2}\int_{-\infty}^{\infty}\int_{-\infty}^{\infty} \phi(\omega_1, \omega_2)e^{-j(\omega_1x_1+\omega_2x_2)}d\omega_1d\omega_2 \tag{23}$$

It is clear that

$$\phi(\omega_1, \omega_2) = E\left[e^{j(\omega_1x_1+\omega_2x_2)}\right]$$

The *joint logarithmic-characteristic function* of x_1 and x_2 is

$$\psi(\omega_1, \omega_2) = \ln\phi(\omega_1, \omega_2) \tag{24}$$

The *marginal* characteristic functions $\phi_{x_1}(\omega) = E\left[e^{j\omega x_1}\right]$ and $\phi_{x_2}(\omega) = E\left[e^{j\omega x_2}\right]$ of x_1 and x_2 can be expressed in terms of their joint characteristic function $\phi(\omega_1, \omega_2)$ as $\phi_{x_1}(\omega) = \phi(\omega, 0)$ and $\phi_{x_2}(\omega) = \phi(0, \omega)$.
The joint moment generation function is given by

$$\phi(s_1, s_2) = E\left[e^{s_1x+s_2x_2}\right]$$

Expanding the exponential and using the linearity of expected values, we obtain the series

$$\begin{aligned}\phi(s_1, s_2) &= \sum_{n=0}^{\infty}\frac{1}{n!}\sum_{n=0}^{n}\left(\begin{array}{c} n \\ k \end{array}\right)E\left[x_1^kx_2^{n-k}\right]s_1^ks_2^{n-k} \\ &= 1 + m_{10}s_1 + m_{01}s_2 + \frac{1}{2}\left(m_{20}s_1^2 + 2m_{11}s_2 + m_{02}s_2^2\right) + \ldots\end{aligned} \tag{25}$$

From this it follows that

$$\frac{\partial^k\partial^r}{\partial s_1^k\partial s_2^r}\phi(0, 0) = m_{kr}$$

The derivatives of the function $\psi(s_1, s_2) = \ln\phi(s_1, s_2)$

$$\frac{\partial^k \partial^r}{\partial s_1^k \partial s_2^r}\psi(0,0) = \kappa_{kr}$$

are by definition the *joint cumulants* κ_{kr} of x_1 and x_2. It can be shown that

$$\kappa_{10} = m_{10}, \quad \kappa_{01} = m_{01}, \quad \kappa_{20} = \mu_{20}, \quad \kappa_{02} = \mu_{02}, \quad \kappa_{11} = \mu_{11} = C_{x_1x_2} = \rho_{x_1x_2}\sigma_{x_1}\sigma_{x_2}$$

2.3.4 Functions of two random variables

Given two random variables x_1 and x_2, and a function $g(x_1, x_2)$, we form a new random variable z as

$$z = g(x_1, x_2)$$

Then, the distribution function $F_z(z)$ may be found as

$$F_z(z_o) = P\{z(\xi) \leq z_o\} = P\{g(x_1, x_2) \leq z_o\} = P\{(x_1, x_2) \in D_z\} = \int\int_{x_1,x_2 \in D_z} f_{x_1x_2}(x_1, x_2)dx_1dx_2$$

where D_z in the x_1x_2 plane represents the region where the inequality $g(x_1, x_2) \leq z$ is satisfied. D_z need not to be simply connected.

The expected value of the random variable $z = g(x_1, x_2)$ is given by

$$E[z] = \int_{-\infty}^{\infty} z f_z(z)dz = \int_{-\infty}^{\infty}\int_{-\infty}^{\infty} g(x_1, x_2)f(x_1, x_2)dx_1dx_2$$

It is straightforward that

$$E\left[\sum_{k=1}^{n} a_k g_k(x_1, x_2)\right] = \sum_{k=1}^{n} a_k E\left[g_k(x_1, x_2)\right] \tag{26}$$

Let $z = x_1 + x_2$. Then, the distribution function can be written as

$$F_z(z) = P\{x_1 + x_2 \leq z\} = \int_{x_1=-\infty}^{\infty}\int_{x=-\infty}^{z-x_2} f_{x_1x_2}(x_1, x_2)dx_1dx_2$$

The probability density function is

$$f_z(z) = \int_{-\infty}^{\infty} f_{x_1x_2}(z - x_2, x_2)dx_2 = \int_{-\infty}^{\infty} f_{x_1x_2}(x_1, z - x_1)dx_1$$

If x_1 and x_2 are independent, then

$$f_{x_1x_2}(x_1, x_2) = f_{x_1}(x_1)f_{x_2}(x_2) \tag{27}$$

and then

$$f_z(z) = \int_{-\infty}^{\infty} f_{x_1}(z - x_2)f_{x_2}(x_2)dx_2 = \int_{-\infty}^{\infty} f_{x_1}(x_1)f_{x_1}(z - x_1)dx_1$$

If two random variables are *independent*, then the density of their sum equals the convolution of their densities. Then,

$$f_z(z) = f_{x_1}(x_1) * f_{x_2}(x_2) \tag{28}$$

2.3.5 Characteristic functions and moments of linear combinations of two random variables.

Let z be a random variable that is a linear combination of two random variables x_1 and x_2

$$z = a_1 x_1 + a_2 x_2$$

The characteristic functions of a linear combination of random variables can be found as follows.

$$\phi_z(\omega) = E\left[e^{j(a_1 x_1 + a_2 x_2)\omega}\right] = \phi(a_1\omega, a_2\omega)$$

If the random variables x_1 and x_2 are independent, then

$$E\left[e^{j(\omega_1 x_1 + \omega_2 x_2)}\right] = E\left[e^{j\omega_1 x_1}\right] E\left[e^{j\omega_2 x_2}\right]$$

From this it follows that

$$\phi(\omega_1, \omega_2) = \phi_{x_1}(\omega_1)\phi_{x_2}(\omega_2) \tag{29}$$

If the random variables x_1 and x_2 are independent and $z = x_1 + x_2$, then

$$E\left[e^{j\omega_1 z}\right] = E\left[e^{j\omega_1 (x_1 + x_2)}\right] = E\left[e^{j\omega x_1}\right] E\left[e^{j\omega x_2}\right]$$

Hence

$$\phi_z(\omega) = \phi_{x_1}(\omega)\phi_{x_1}(\omega) \quad ; \quad \psi_z(\omega) = \psi_{x_1}(\omega) + \psi_{x_1}(\omega)$$

In this case, the moments n order of z are:

$$m_{z,n} = E[z^n] = E[(a_1 x_1 + a_2 x_2)^n]$$

the term in the parentheses above is the well known Newton binomial

$$(a_1 x_1 + a_2 x_2)^n = \sum_{j=0}^{n} C_n^j (a_1 x_1)^{n-j} (a_2 x_2)^j$$

where

$$C_n^j = \frac{n!}{j!(n-j)!}$$

and, therefore,

$$m_{z,n} = \sum_{j=0}^{n} C_n^j a_1^{n-j} a_2^j m_{(n-j)j} \tag{30}$$

where $m_{(n-j)j} = E[x_1^{n-j} x_2^j]$ is the joint moment of orders $(n-j)$ and j of the variables x_1 and x_2. The central moments of order n of z can be also be written as:

$$\mu_{z,n} = E[(z - \eta_z)^n] = E[(a_1 x_1 + a_2 x_2 - \eta_z)^n]$$

where η_z is the mean of the variable z, and can be written as $\eta_z = a_1\eta_1 + a_2\eta_2$, where η_1 and η_2 are the means of the random variables x_1 and x_2. Therefore,

$$\mu_{z,n} = E[(z - \eta_z)^n] = E[(a_1(x_1 - \eta_1) + a_2(x_2 - \eta_2))^n]$$

that can be also developed as the Newton binomial and, hence,

$$\mu_{z,n} = \sum_{j=0}^{n} C_n^j a_1^{n-j} a_2^j \mu_{(n-j)j} \tag{31}$$

It could be also demonstrated (see [10]) that

$$\kappa_{z,n} = \sum_{j=0}^{n} C_n^j a_1^{n-j} a_2^j \kappa_{(n-j)j} \tag{32}$$

where $\kappa_{z,n}$ is the cumulant of order n of the variable z, and $\kappa_{(n-j)j}$ is the joint cumulant of order $(n-j)$ and j of the variables x_1 and x_2

When x_1 and x_2 are independent, these equations can be expressed in an easier way as:

$$m_{z,n} = a_1^n m_{n,0} + a_2^n m_{0,n} \tag{33}$$

$$\mu_{z,n} = a_1^n \mu_{n,0} + a_2^n \mu_{0,n} \tag{34}$$

$$\kappa_{z,n} = a_1^n \kappa_{n,0} + a_2^n \kappa_{0,n} \tag{35}$$

2.3.6 Moments of linear combination of several random variables.

When there are more than two random variables, it is difficult to generalize the notation used in the previous section. In these cases it is better to denote the moments and cumulants in the following way. Let Y be a vector of random variables that are transformed from a set of random variables X as

$$Z = AX$$

or $z_r = a_{ri} x_i$, where the subscripts specify the variable in the sets.

The joint moment of second order of the variables x_i and x_j will be called m_x^{ij}. The joint cumulant of order three of the variables x_i, x_j and x_k will be called κ_x^{ijk},and so on. The indices i, j and k can be equal.

Then, the equations (30), (31) and (32) can be written for the cumulants of order 3, for instance, as

$$\kappa_z^{rst} = \sum_i \sum_j \sum_k a_{ri} a_{sj} a_{tk} \kappa_x^{ijk} \tag{36}$$

It can be easily verified that equation (36) gives the same results than equation (32), for the third order moments, and two variables.

Similar equations could be written, as in the previous sections, for moments. However, it is better to work with cumulants for the following reasons [10]:

- Most statistical calculations using cumulants are simpler than the corresponding calculation using moments.
- For independent random variables, the cumulants of a sum are the sum of cumulants.
- For independent random variables, the cross-cumulants are zero.
- Series expansion, such as the Cornish-Fisher expansion are most conveniently expressed using cumulants.
- Where approximate normality is involved, high order cumulants can usually be neglected, but not higher order moments.

2.4 Generation of correlated random numbers

This section shows how to generate multivariate dependent random numbers. The way of modelling this dependence is through the correlation matrix. Although the approach shown here is not able to reproduce the dependence among variables with total accuracy, due to the nonlinearity of the process, the method is accurate enough for a first approach. The method has been thought for being used in MATLAB, that from the multivariate normal distribution, makes possible to generate random numbers with, as said, any other marginal distribution, even different among them.

The fundamental of the method is the inverse transformation of a uniform distribution. Let x_1 be a random variable with uniform distribution $U(0,1)$. Let $x_{1,k}$ be the sample k of the $U(0,1)$. Then, to generate random numbers of a given distribution with CDF $F(x)$, $x_{2,k}$, it is necessary to perform the simple operation $x_{2,k} = F^{-1}(x_{1,k})$. If we transform this new variable, forming $x_{3,k} = F(x_{2k})$, then x_{3k} will have a $U(0,1)$ distribution.

The method begins by generating random numbers of a multivariate normal random variable, with a given correlation matrix, forming the array $\mathbf{x}_1$, where there are as many rows as variables, and as many columns as numbers desired, or samples. Each element could be written as $x_{1,ij}$, where i is the variable, and j the sample. Then, a normal transformation is made to this values in order to obtain a multivariate uniform distribution, $\mathbf{x}_2$. $\mathbf{x}_2 = F(\mathbf{x}_2)$, where $F(\mathbf{x})$ is a multivariate normal CDF.

The third step consists in transforming the obtained marginal distributions in the wished distribution G. Then, the sample j of the new variable i $x_{3,ij}$ will be obtained as $x_{3,ij} = G^{-1}(x_{2,ij})$.

These transformations, however, being nonlinear, do not keep the exact value of the correlation coefficient, although the new correlation coefficient is quite close to it. More complex methods, such as copula modeling could be used to preserve the desired correlation among variables, that is in the origin of the transformations.

2.5 Approximation of distribution functions.

The problem that is going to be considered here is how to obtain a distribution (or density) probability function, given its moments or cumulants. Different approaches have been made, some of them based on series expansions that obtain the PDF in terms of a base function.

2.5.1 Gram-Charlier A series.

Let consider the series expansion of a probability density function $f(x)$ with mean $\eta = 0$ and $\sigma = 1$ in terms of a base function $\varphi(x)$, where $\varphi(x)$ is N(0,1). This expansion may be written as:

$$f(x) = \sum_{j=0}^{\infty} c_j \varphi^{(j)}(x) \tag{37}$$

where $\varphi^{(j)}(x)$ is the j-th derivate of $\varphi(x)$. This equation may be written in terms of the Tchebycheff-Hermite polynomials (see Appendix B), H_j as,

$$f(x) = \sum_{j=0}^{\infty} c_j H_j \varphi(x) \tag{38}$$

multiplying by $H_r(x)$ and integrating from $-\infty$ to ∞ we have, in virtue of the orthogonal relationship between Tchebycheff-Hermite polynomials

$$c_r = \frac{1}{r!} \int_{-\infty}^{\infty} f(x) H_r(x) dx \tag{39}$$

From equation (39), the values of c_r may be obtained as funcions of the central moments μ. The first terms are:

$$\begin{aligned}
c_0 &= 1 \\
c_1 &= 0 \\
c_2 &= 0 \\
c_3 &= \frac{1}{3!}\mu_3 \\
c_4 &= \frac{1}{4!}(\mu_4 - 3) \\
c_5 &= \frac{1}{5!}(\mu_5 - 10\mu_3) \\
c_6 &= \frac{1}{6!}(\mu_6 - 15\mu_4 + 30) \\
c_7 &= \frac{1}{7!}(\mu_7 - 21\mu_5 + 105\mu_3) \\
c_8 &= \frac{1}{8!}(\mu_8 - 28\mu_6 + 210\mu_4 - 315)
\end{aligned}$$

A distribution with variance σ^2 should be normalized, and the values μ_r in the previous equation should be changed to $\frac{\mu_r}{\sigma^r}$.

This is the so-called Gram-Charlier series of Type A.

It can be demonstrated [15] that this infinite series converges if the integral

$$\int_{-\infty}^{\infty} e^{\frac{x^2}{4}} dF(x) \tag{40}$$

converges and if $f(x)$ tends to zero as $|x|$ tends to infinity. This limits the valid distributions only to a reduced number of the most common distributions. From the statistical viewpoint, however, the important question is not whether an *infinite* series can represent a frequency function, but whether a finite number of terms can do so to a satisfactory approximation. It is possible that even when the infinite series diverges, its first few terms will give an approximation of an asymptotic character. Actually, the series in the Charlier form may behave irregularly in the sense that the sum of k terms may give a worse fit than the sum of $(k-1)$ terms. In many statistical inquiries we are more interested in the tails of a distribution than its bejaviour in the neghbourhood of the mode, and it is here that the Type A series appears particularly inadequate (see [11]).

2.5.2 The Cornish-Fisher expansion.

The Cornish-Fisher expansion (see [13], [16] [17] for details) provides an approximation of a quantile α of a distribution function $F(x)$ in terms of the quantile of a normal $N(0,1)$ distribution Φ and the cumulants of $F(x)$. Using the first five cumulants, the expansion is [19], [11],

$$\begin{aligned}
x(\alpha) \approx\ & \xi(\alpha) + \frac{1}{6}(\xi^2(\alpha) - 1)\kappa_3 + \frac{1}{24}(\xi^3(\alpha) - 3\xi(\alpha))\kappa_4 \\
& -\frac{1}{36}(2\xi^3(\alpha) - 5\xi(\alpha))\kappa_3^2 + \frac{1}{120}(\xi^4(\alpha) - 6\xi^2(\alpha) + 3)\kappa_5 \\
& -\frac{1}{24}(\xi^4(\alpha) - 5\xi^2(\alpha) + 2)\kappa_3\kappa_4 + \frac{1}{324}(12\xi^4(\alpha) - 53\xi^2(\alpha) + 17)\kappa_3^3
\end{aligned} \tag{41}$$

where $x(\alpha) = F^{-1}(\alpha)$ and $\xi(\alpha) = \Phi^{-1}(\alpha)$ and κ_r is the cumulant of orden r of the distribution function F.

Although the convergence properties of Cornish-Fisher series are difficult to demonstrate [17], and are somehow related to Gram-Charlier series, their behavior for non-Gaussians PDF is better than the latter, as shown below.

2.5.3 Comparison between Gram-Charlier and Cornish-Fisher expansions.

As explained before, Gram-Charlier A series converge with difficulties to non-Gaussian functions, and numerical errors may even make worse this convergence, as noted by [12].

For instance, the reconstruction of the cumulative density function (cdf) of a Weibull ($a = 2$ and $b = 2$) distribution when 6 terms of the Gram-Charlier series are considered, is given in the figure 1. It can be seen that the fitting is bad. If more terms of the series are used, the result is even worse.

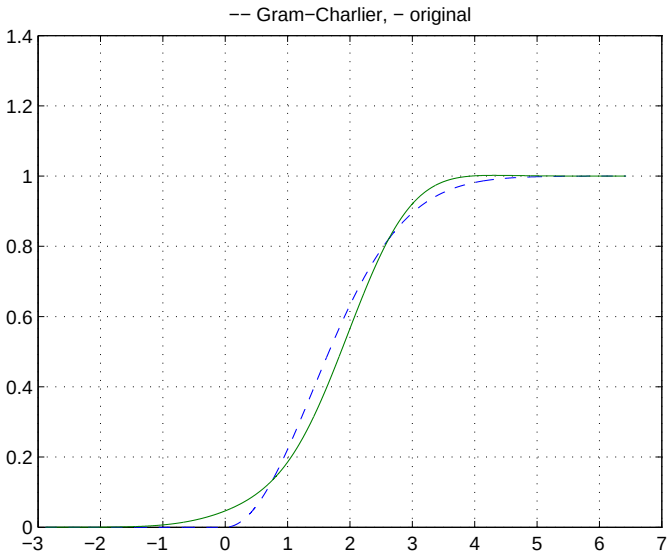

Figure 1: Reconstruction of a Weibull cdf using Gram-Charlier expansions. $a = 2$, $b = 2$.

The same approximation, using the Cornish-Fisher expansion yields Figure 2. It can be seen that the approximation is better.

A numerical comparison may be made between both approximations. This comparison will be performed to the tail values, since they are the most important for system security analysis. For this case, the values for the .9 and .95 values of the original CDF and the approximations is given in table 1. The values are expressed as a fraction of the distribution mean.

	Gram-Charlier		Cornish-Fisher	
	6 terms	4 terms	11 terms	6 terms
.9	0.1015	0.064	.0331	.0571
.95	.1595	.1557	.0733	.1058

Table 1: Comparison between Cornish-Fisher and Gram-Charlier approximations. Values in p.u. of the mean.

In this table, it can be noticed that the accuracy of the Cornish-Fisher approximation is better than the Gram-Charlier series. Besides, the accuracy of the latter is smaller if more terms are used, while the former increases it with the number of terms. For both approximations, the error is greater when they consider values closer to the distribution tail.

2.5.4 Multimodal distributions.

A multimodal distribution is a distribution of a random variable with several modes. A multimodal distribution comes from a combination of a continuous and a discrete random variables.

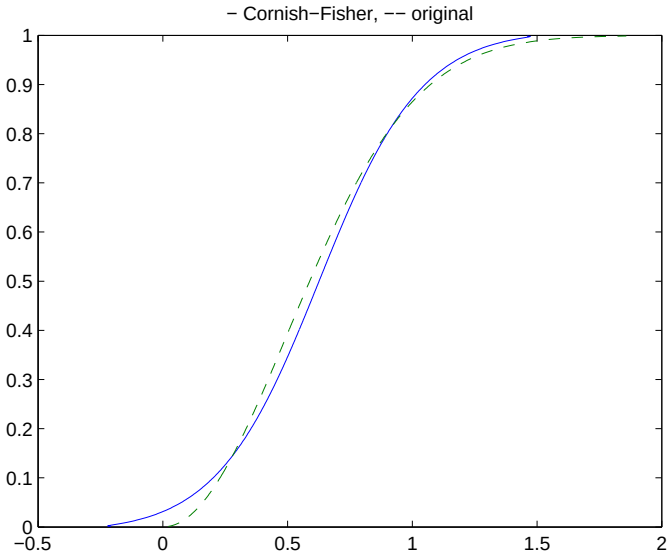

Figure 2: Reconstruction of a Weibull cdf using Cornish-Fisher expansions. $a = 2$, $b = 2$.

In the case of a multimodal distribution, to know the values of the moments ais not enough to estimate the PDF or CDF of the random variable through series expansion. The percentiles of the function cannot be, hence, properly estimated either by this means.

An example of multimodal CDF compared with a unimodal CDF with the same moments is given in Figure 3.

In the following approach a linear combination of variables will be considered. Let z be a linear combination of the discrete variable x_d and the continuous variable x_c. Both variables are independent. Then,

$$z = x_c + a_d x_d$$

where a_d is a real constant. The most obvious approach to the estimation of the PDF of z is the convolution of those variables (see section 2.3.4), since they are independent.

It is a well known property of the Fourier transform that the transform of a convolution of two functions is the product of their Fourier transform. Therefore,

$$f_z(z) = f_{x_1}(x_1) * f_{x_2}(x_2) \quad \leftrightarrow \quad \mathcal{F}_z(\omega) = \mathcal{F}_{x_1}(\omega) \cdot \mathcal{F}_{x_2}(\omega)$$

Where $\mathcal{F}$ stands for the Fourier transform of f. It must be recalled that the Fourier transform of a discrete function renders a periodic function in the complex domain. An example of a transform of a continuous PDF, a discrete PDF, and its product is given in Figure 4. An exponential and a binomial distributions have been chosen. The result of the convolution is given in Figure 5. It can be seen that the transform of the discrete distribution is a periodic function.

Not all linear combinations of discrete and continuous variables render z a multimodal distribution. This depends on the nature of both, and on the coefficient a_d. For instance, the functions whose transforms are given in Figure 6, render the PDF shown in Figure 7, which is unimodal. In this example, the continuous PDF is a normal, while the discrete random variables has a binomial distribution.

Since the convolution is a computationally expensive procedure, if there are many discrete variables and many combinations to be considered, the computational burden increases hugely. Therefore, it is interesting to determine under which conditions the convolution of a discrete and a continuous variables would yield a multimodal PDF in order to reduce the number of convolutions as much as possible. When the distribution is unimodal, the Cornish-Fisher series expansion gives a good approximation, as if it

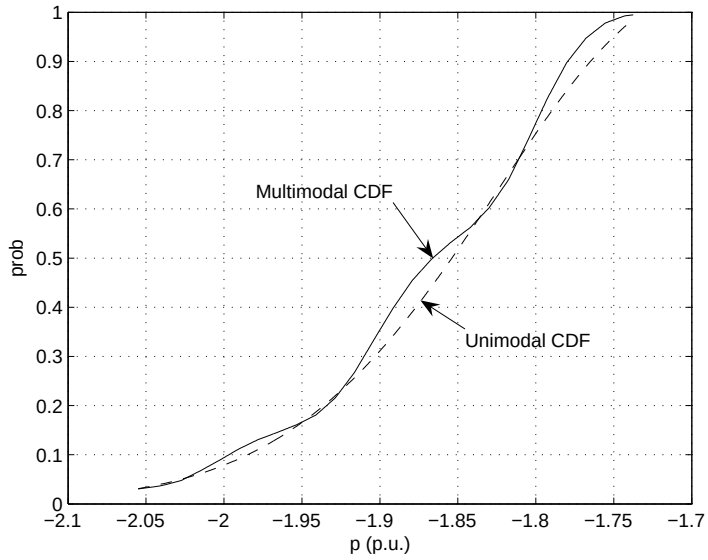

Figure 3: Multimodal and unimodal CDF with the same moments.

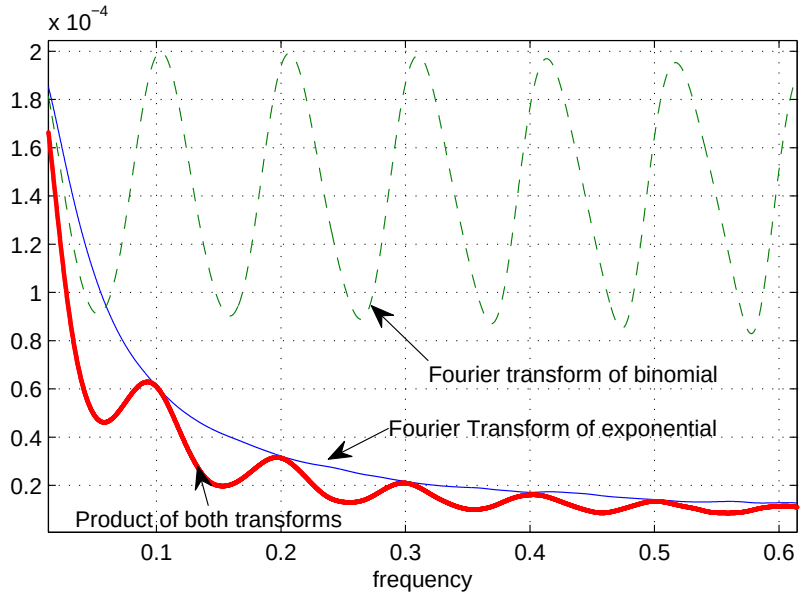

Figure 4: Transforms of a discrete and continuous PDF, and their product. Multimodal case.

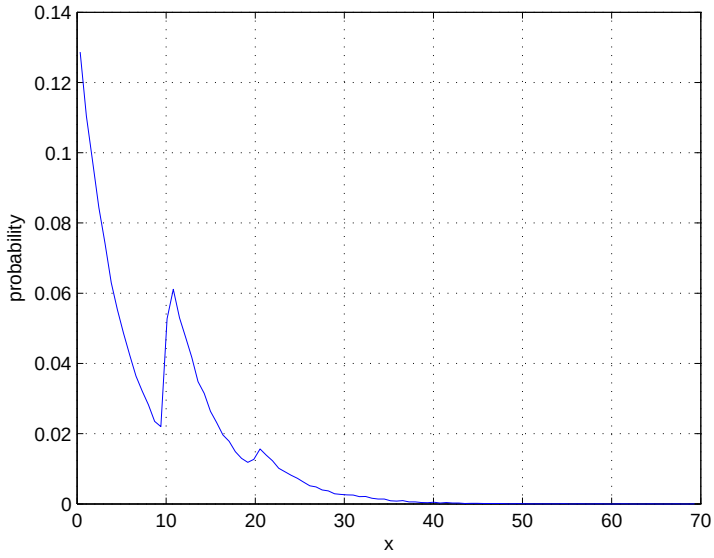

Figure 5: Multimodal PDF from a combination of a discrete and continuous functions.

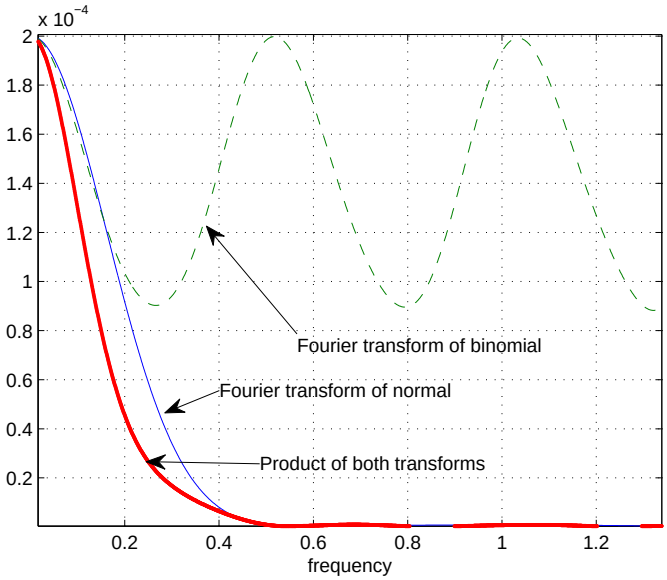

Figure 6: Transforms of a discrete and continuous PDF, and their product. Unimodal case.

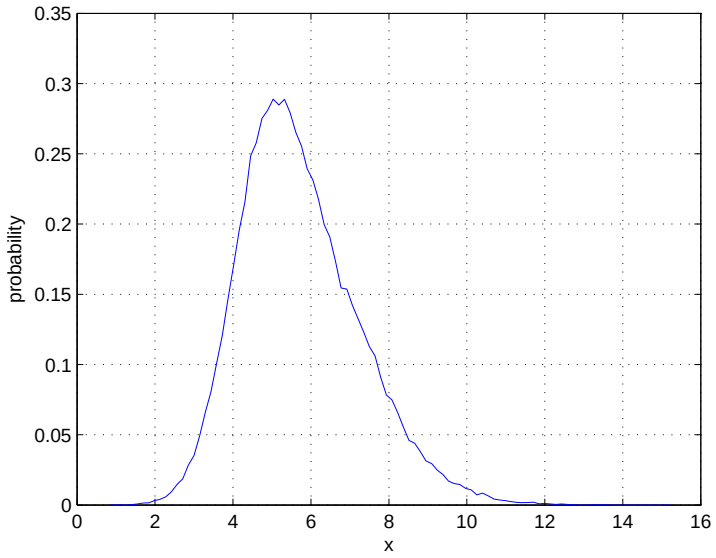

Figure 7: Unimodal PDF from a combination of a discrete and continuous functions.

were a linear combination of continuous variables. In practice, only a limited number of convolutions is necessary.

To obtain the condition for a multimodal distribution, it is better to work in the frequency domain, as can be expected from the previous figures. This condition is that the transform of the continuous variable has a sufficiently low value at the frequency of the, say, second peak of the Fourier transform of the discrete variable. This peak is given by

$$f_{lim} = \frac{1}{a_d \Delta x_d}$$

where Δx_d is the separation between two non zero values of the discrete distribution. Therefore, the unimodality condition is:

$$|\mathcal{F}_c(f_{lim})| < \varepsilon_f \tag{42}$$

Where ε_f is a number sufficiently small and $\mathcal{F}_c$ is the Fourier transform of the continuous function. If this condition is fulfilled, then the result of the convolution would be an unimodal function, and a Cornish-Fisher expansion would render a good approximation. Otherwise, a convolution should be performed.

3 Short term wind power prediction. Uncertainty.

3.1 Short term wind power prediction.

Short term wind power prediction programs are tools that provide an estimation of the future power production of a wind farm, or a group of wind farms, in the next hours. For this purpose, they use meteorological forecasts coming from a Numerical Weather Prediction (NWP) tool, and sometimes real time SCADA data from the wind farms, as wind power production, measured wind speed, etc. Data of the wind farms, such as rated power, type and availability of wind turbines, etc. are also necessary. The output of these programs is the hourly average wind farm production for the next hours. Typically, predictions are issued for the next 48 hours, but longer time horizons are possible, sometimes at the price of a lower accuracy.

These predictions tools are less accurate than load prediction programs and their accuracy decreases with the time horizon. A survey of the accuracy of these tools is given in [25], and an example for a typical wind farm, where the output from the prediction program SIPREOLICO is compared to persistence is shown in Figure 8. Persistence is a prediction method that assumes that the future production, for the entire time horizon considered, is the current production of the wind farm, i.e. $\widehat{p}(t+k|t) = p(t)$, where $\widehat{p}(t+k|t)$ is the power predicted at time t for k hours later, and $p(t)$ is the wind farm generated power at time t. This method is considered as a threshold of the performance of a forecasting method. SIPREOLICO is a prediction program used since year 2002 in Red Eléctrica de España, the Spanish TSO, and developed by Universidad Carlos III de Madrid, to forecast wind power production of the next 42 hours, every 15 minutes, for the 14 GW of wind power connected to the Spanish peninsular grid. Details of SIPREOLICO can be found in [26].

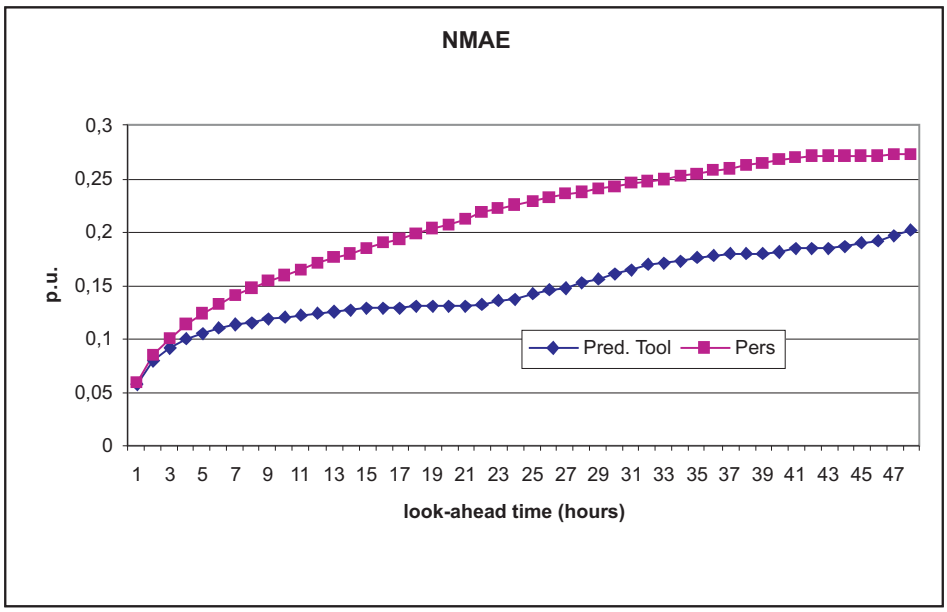

Figure 8: NMAE of SIPREOLICO and persistance for a typical wind farm.

Figure 8 represents the Normalized Mean Average Error, defined as

$$NMAE(k) = \frac{1}{P_n} \frac{\sum_{t=1}^{N} |e(t+k|t)|}{N} \tag{43}$$

Where

$$e(t+k|t) = p(t+k) - \widehat{p}(t+k|t)$$

And $p(t+k)$ is the production of the wind farm at time $(t+k)$. P_n is the nominal power of the wind farm, and N is the number of predictions examined along the considered time. It can be seen that the wind power prediction accuracy allows for much uncertainty, and that the actual value may differ widely from the predicted one.

3.2 Uncertainty of short term wind power prediction.

The predictions provided by a short term wind power prediction program are uncertain, and it is interesting to estimate this uncertainty in order to have more information about the future production of a wind farm. Let p be the random variable associated with the power output of a wind farm. Then, the probability of producing p MW, having predicted $\widehat{p}$ MW k hours before, is given by the probability density function $f_{\widehat{p},k}(p)$. The uncertainty, and hence the probability density function, changes with the

range of the wind farm power otuput, since this value is bounded between zero and the rated power. Besides, the power curve of a wind turbine or wind farm is nonlinear. If we assume that the wind speed predictions have gaussian uncertainty, then the probability density functions of the power predictions will not be gaussian. The shape of these probability density functions is also affected by the time lag elapsed between the prediction and the operation times. As shown before, predictions with a shorter time lag are more accurate, and the variance of their uncertainty distribution is likely to be smaller than those predictions produced longer before. To obtain analytically, or in real time, the uncertainty of this prediction is difficult, but accurate estimations can be made from past data, and some research has already been made in this field. Given the past predictions and wind production for these predictions, the accuracy of these predictions can be tabulated, and then their frequency can be used as an approximation of these probability density functions. If the power range of a wind farm is comprised between 0 and P_{max}, and this range is divided in Q intervals, the power p would be included in the interval q, if

$$\frac{q-1}{Q}P_{max} \leq p \leq \frac{q}{Q}P_{max}$$

The probability density function $f_{\widehat{p},k}(p)$ changes into $f_{\widehat{q},k}(p)$, where $\widehat{q}$ is the interval in which the predicted power $\widehat{p}$ is included. As an example, the following figures give the frequency distributions of the produced powers for different values and time lags of the prediction. Figure 9 shows the frequency distribution when a low power had been predicted 7 hours before real time, while Figure 11 shows the frequency distribution when the power level is near the average. All these values have been obtained from real production of three months of a wind farm whose rated power has been normalized to 1.

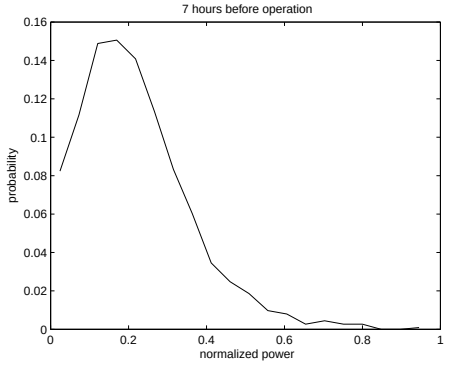

Figure 9: $f_{\widehat{q},k}(p)$ for $q* = 2$ and $k = 7$. $Q = 14$.

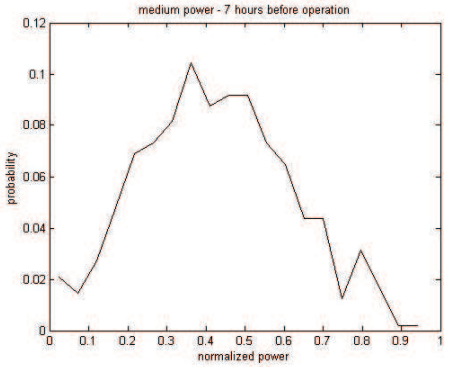

Figure 10: $f_{\widehat{q},k}(p)$ for $\widehat{q} = 7$ and $k = 7$. $Q = 14$.

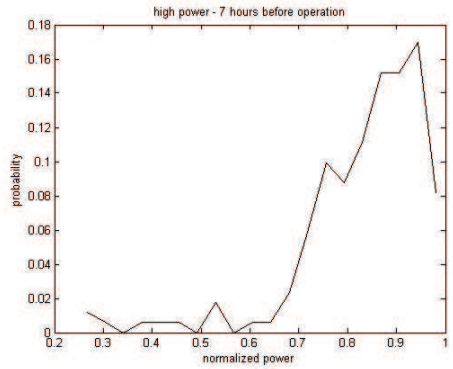

Figure 11: $f_{\widehat{q},k}(p)$ for $\widehat{q} = 13$ and $k = 7$. $Q = 14$.

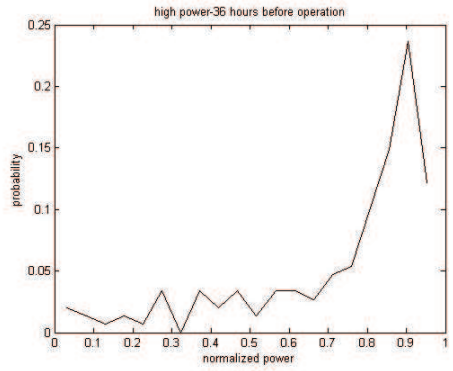

Figure 12: $f_{\widehat{q},k}(p)$ for $\widehat{q} = 13$ and $k = 36$. $Q = 14$.

It is not the purpose of this work to propose a model for this uncertainty, and a reasonable assumption will be used as an approximation. Due to the bounded nature of the power produced by a wind farm, a Beta PDF will be used, as proposed in [27]. Heuristic PDF, as shown in [28], supports this assumption, although this is still an open field for research. The Appendix D.1 gives the analytical expression of Beta distribution. In our case, the mean of the distribution will be the predicted power at the time of interest, while the standard deviation σ will depend on the level of power injected, with respect to the wind farm rated power. This dependence has been obtained heuristically for some wind farms, and the results are shown in Figure 13, where the value of standard deviation is normalized to the rated power of the wind farm. Although there are wide variations, an approximation by a quadratic curve (shown in the picture) will provide realistic results.

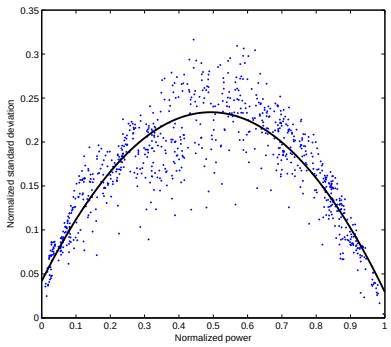

Figure 13: Relation between standard deviation and mean for the uncertainty of predictions.

The uncertainty of short term wind power prediction of geographically close wind farms are correlated, since the wind power in all of them are due to similar meteorological simulations. This dependence has not been modeled up to now, but the studies such as [18] show the dependence between productions in a wide area (Germany). These results may be considered as an estimation of actual correlation values, although it is necessary to wait until more specific studies are made.

4 Load flow equations.

In order to give the notation used in the probabilistic load flow, the load flow equations will be recalled here. Two general formulations will be given, DC and AC, and in the last case the linear sensitivities of the line flows to the nodal power injections with distributed slack bus will be found.

4.1 DC load flow.

The well-known DC load flow equations are:

$$\begin{aligned} \mathbf{B}'\delta &= \mathbf{P} \\ \mathbf{P}_f = \mathbf{X}^{-1}\mathbf{T}^t &= \mathbf{X}^{-1}\mathbf{T}^t\mathbf{B}'^{-1}\mathbf{P} = \mathbf{A}\mathbf{P} \end{aligned} \tag{44}$$

Where $\mathbf{P}_f$ is the vector of power flows through lines, $\mathbf{P}$ is the vector of net nodal power injections, $\mathbf{B}'$ is the susceptance matrix whose terms are $B_{ij} = -1/X_{ij}$, $B_{ii} = \sum_{i \neq j} 1/X_{ij}$ and δ is the vector of nodal voltage angles, $\mathbf{X}^{-1}$ is a diagonal matrix whose terms are the inverse of the branch reactances, $\mathbf{T}$ is the branch-node incidence matrix, and $\mathbf{A} = \mathbf{X}^{-1}\mathbf{T}^t\mathbf{B}'^{-1}$ is the coefficient matrix that relates the line power flows to the nodal power injections. This establishes the linear relation between power flows and nodal power injections.

For this purpose the DC load flow equations provide a good estimate of the power flows. Figure 14 shows the relative error in % of power flows in lines between AC and DC solution. This has been calculated for all the lines in the Transmission network of the Peninsular Spanish Power system, for 72

representative cases along year 2004. The minimum power limit of the lines in the studied case is around 220 MW. Beyond this power, the error is less than 5% between DC and AC power flows. Therefore, for large powers (with risk of overload, or congestion) the errors are small enough, so DC load flow can be considered as an adequate first approximation, at least as a approach.

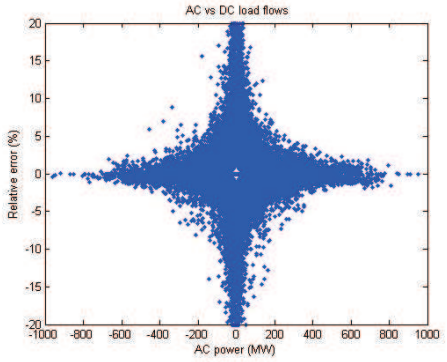

Figure 14: Comparison between AC and DC load flows in the Spanish peninsular transmission grid.

4.2 Linearization of AC load flow equations.

Let us write the nonlinear load flow equations for a power system as:

$$\begin{aligned} \mathbf{S} &= \mathbf{g}(\mathbf{Z}) \\ \mathbf{P_f} &= \mathbf{h}(\mathbf{Z}) \end{aligned} \tag{45}$$

Where $\mathbf{Z}$ is the vector of nodal voltages and angles, $\mathbf{S}$ is the input vector of real and reactive power injections, and $\mathbf{P_f}$ is the output vector of line active power flows; $\mathbf{g}$ and $\mathbf{h}$ are nonlinear functions. Linearizing these equations around a working point yields, after some calculation,

$$\Delta\mathbf{P_f} = \mathbf{J_h}\mathbf{J_P}^{-1}\Delta\mathbf{P} = \mathbf{\Lambda_f}\Delta\mathbf{P} \tag{46}$$

$\Delta\mathbf{P}$ is the vector of active power injections taken from vector $\mathbf{S}$. $\mathbf{J_h}$ is the jacobian matrix of nonlinear function $\mathbf{h}$, while $\mathbf{J_P}$ is the submatrix of the jacobian matrix of function $\mathbf{g}$ that relates line active power flows to state variables. Reactive power injections have not been considered because of the low interaction between reactive power injections and active power flows, and because modern wind generation tend to control the reactive power injections due to economic incentives. Therefore, variations of reactive power injected by wind farms may be overlooked. The power factor of loads will be considered constant, and hence the changes in the reactive power demanded are just proportional to the active power.

Matrix $\mathbf{\Lambda_f}$ is, therefore, a sensitivity matrix whose terms are the system Power Transfer Distribution factors (PTDF). The definition of these PTDF assumes that the power injections are compensated by opposite power injections at the slack bus. This could be an acceptable assumption when the injections have a small value. However, large fluctuations due to variation of power in wind farms may be compensated by the combined operation of several generators. For this reason, the sensitivity coefficients used in this work have been calculated considering a distributed slack bus. Evidently, conventional PTDF are a particular case of this scheme. The new sensitivities can be easily calculated in the following way.

Let be ΔP_1 and ΔP_2 the injected power of two wind farms, and ΔP_3 and ΔP_4 the compensation of the regulating generators. Then, the linear approximation to the flow in a line, ΔP_f is:

$$\Delta P_f = \lambda_1\Delta P_1 + \lambda_2\Delta P_2 - \lambda_3\Delta P_3 - \lambda_4\Delta P_4$$

Let us call $\Delta P = \Delta P_1 + \Delta P_2 = \Delta P_3 + \Delta P_4$. Then, the power injected by the regulating generators would be $\Delta P_3 = k_3 \Delta P$, and $\Delta P_4 = k_4 \Delta P$

The power increase in the considered line could be written as:

$$\Delta P_f = \lambda_1 \Delta P_1 + \lambda_2 \Delta P_2 - (k_3 \lambda_3 + k_4 \lambda_4) \Delta P$$

or

$$\Delta P_f = (\lambda_1 - (k_3 \lambda_3 + k_4 \lambda_4)) \Delta P_1 + (\lambda_2 - (k_3 \lambda_3 + k_4 \lambda_4)) \Delta P_2$$

or, in general,

$$\Delta P_f = \sum_j \left(\lambda_j - \sum_{r=1}^{R} k_r \lambda_r \right) \Delta P_j$$

Hence, the new sensitivity coefficients, with the distributed slack bus are defined as:

$$\lambda'_{qi} = \lambda_{qi} - \sum_{r=1}^{R} k_r \lambda_{qr} \tag{47}$$

Where λ_{qi} is the term (q, i) of the sensitivity matrix $\mathbf{\Lambda_f}$, that is to say, the PTDF of line q with respect to an injection in node i, k_r is the part of power injection in node i that the regulating generator r assumes, as defined previously, for example $\left(k_r = \frac{1}{R}\right)$. R is the number of generators that compensate the injection in node i. Of course, any other sharing of load variation among generators is possible, and even economic criteria could be considered. Finally, it may be written that

$$\mathbf{\Delta P_f} = \mathbf{\Lambda'_f} \mathbf{\Delta P} \tag{48}$$

Where ΔP includes only the considered power injections, i.e., the random power injections in our case.

A similar approach may be made for the estimation of reactive power and voltage. The accuracy of these approximations would be, however, smaller. This approximation can be written as (49).

$$\mathbf{\Delta Q_f} = \mathbf{\Gamma'_f} \mathbf{\Delta P} \tag{49}$$

5 Probabilistic load flow.

Probabilistic power flow is a tool that provides the probability of a system variable taking a value. These variables may be node voltages, or power through lines, or any other. The aim of this program is to estimate the risk of line overloading and congestion for the next hours.

In the following sections, the fundamentals and practical implementation of two different proposed methods will be described. Firstly, the point estimate method, that has been recently proposed to solve this problem. Then, a method that make use of the properties of a linear combination of random variables and will be called *Enhanced Linear Method* (ELM). To do this, it is necessary to use a linear approximation of the load flow equations.

Point estimate method are useful for independent power injections, but become very cumbersome for dependent random variables. ELM can be used both for dependent and independent variables, and its implementation will be described in three steps. First, the method for independent variables, only with continuous distributions of the random variables, and using DC load flow (ELM-IDC) will be explained. Then, the method for dependent continuous random variables (ELM-C) will follow. Finally, the more general case with continuous and discrete dependent variables will be described (ELM).

In both cases, the final result of these methods are the moments of the distribution of the power flows and other system variables. It is necessary to estimate the CDF of the resulting magnitudes to know the probability of the line flow to surpass the line flow limits. Thus, a method should be used to build this CDF from the obtained moments. These methods have been described in previous sections, and they will be Cornish-Fisher expansion series and convolution when necessary. Their accuracy in achieving this task will be evaluated in next sections.

5.1 Point estimate methods.

Point estimate methods have been recently proposed for the load flow problems in the works of [4] and [30]. The next sections explains the fundamental of the method, and its practical implementation.

5.1.1 Independent random variables.

Functions of one variable. Let x be a random variable with probability density function $f_x(x)$, and $z = h(x)$. The moment of order n of variable x will be called $m_{x,n}$, and the central moment of order n $\mu_{x,n}$. The mean of x will be $\eta_x = m_{x,1}$ and its variance $\sigma_x^2 = \mu_{x,2}$. Let's call

$$\lambda_{x,n} = \frac{\mu_{x,n}}{\sigma_x^n}$$

Then, $\lambda_{x,1} = 0$, $\lambda_{x,2} = 1$ and $\lambda_{x,3}$ and $\lambda_{x,4}$ are the skewness and kurtosis coefficients respectively.
If we write the Taylor expansion series of $z = h(x)$ around its mean η_z, we get the following expression:

$$h(x) = h(\eta_z) + \sum_{n=1}^{\infty} \frac{1}{n!} h^{(n)}(\eta_x)(x - \eta_x)^n$$

where $h^{(n)}(\eta_x)$ means the derivative of order n of the function $h(x)$ evaluated at η_x.
Then, the value of η_z may be also obtained as:

$$\begin{aligned} \eta_z &= E[h(x)] = \int_{-\infty}^{\infty} h(x) f_x(x) dx \\ &= h(\eta_z) + \sum_{n=1}^{\infty} \frac{1}{n!} h^{(n)}(\eta_x) \mu_{x,n} \\ &= h(\eta_z) + \sum_{n=1}^{\infty} \frac{1}{n!} h^{(n)}(\eta_x) \lambda_{x,n} \sigma_x^n \end{aligned} \tag{50}$$

The point estimate method intents to approximate the mean (and higher order moments) by a linear combination of the value of function h in several points. For two points, x_1 and x_2 this approximation can be written as:

$$\eta_z \simeq p_1 h(x_1) + p_2 h(x_2)$$

where $x_1 = \eta_x + \xi_1 \sigma_x$ and $x_2 = \eta_x + \xi_2 \sigma_x$ and p_1 and p_2 are the weights to be found, together with the values of ξ_1 and ξ_2. The approximation may be written as

$$\eta_z \simeq p_1 h(x_1) + p_2 h(x_2) = h(\eta_x)(p_1 + p_2) + \sum_{n=1}^{\infty} \frac{1}{n!} h^n(\eta_x)(p_1 \xi_1^n + p_2 \xi_2^n) \sigma_x^n \tag{51}$$

since

$$h(x_i) = h(\eta_z) + \sum_{n=1}^{\infty} \frac{1}{n!} h^{(n)}(\eta_x)(x_i - \eta_x)^n$$

and $x_i = \eta_x + \xi_i \sigma_x$. Since there are four unknowns, four equations are necessary to find them. These equations are obtained equalling the first four terms of the series developments (50) and (51):

$$\begin{aligned} p_1 + p_2 &= 1 \\ p_1 \xi_1 + p_2 \xi_2 &= 0 \\ p_1 \xi_1^2 + p_2 \xi_2^2 &= 1 \\ p_1 \xi_1^3 + p_2 \xi_2^3 &= \lambda_{x,3} \end{aligned} \tag{52}$$

The solution to this system is, [24],

$$\begin{aligned} \xi_j &= \frac{\lambda_{x,3}}{2} + (-1)^{3-j}\sqrt{1+\left(\frac{\lambda_{x,3}}{2}\right)^2} \\ p_j &= (-1)^j \frac{\xi_{(3-j)}}{\zeta} \end{aligned} \tag{53}$$

where

$$\zeta = \xi_1 - \xi_2 = 2\sqrt{1+\frac{\lambda_{x,3}}{2}}$$

since the third first terms of the series development of η_z have been equalled, it is a third order approximation

$$\eta_z = p_1 h(x_1) + p_2 h(x_2) + \sum_{n=4}^{\infty} \frac{1}{n!} h(\eta_z)^{(n)} (\lambda_{x,n} - (p_1 \xi_1^n + p_2 \xi_2^n)) \sigma_x^n$$

A similar way can be used to approximate higher order moments, for instance,

$$E[z^2] \simeq p_1 h(x_1)^2 + p_2 h(x_2)^2$$

This method can be extended to more points. This implies a higher order approximation to the moments.

Functions of several variables. Let z be a random variable that is a funcion of several independent random variables, $z = h(\mathbf{x})$, where $\mathbf{x} = (x_1, \ldots, x_n)$. The probability density functions of each variable x_k will be $f_k(x_k)$, and the joint probability density function will be $f_x(x_1 \ldots, x_n)$, and $\frac{\partial^{(kn)} f_x}{\partial x_{k1} \ldots \partial x_{kn}} = 0$, if $\exists\ ki \neq kj$. $\mu_{k,n}$ will be the central moment of order n of the variable x_k, whose mean and variance are η_k and $\sigma_k^2 = \mu_{k,2}$.

Let consider the points $x_{k,i} = \eta_k + \xi_{k,i}\sigma_k$ for $i = 1, \ldots, m$ points and $k = 1, \ldots, n$ variables. Each point will be associated to a weight $p_{k,i}$ such that $\sum_{k=1}^{n} \sum_{i=1}^{m} p_{k,i} = 1$.

Then, $z = h(\mathbf{x})$ can be expanded in multivariate Taylor series around the point $\eta_{\mathbf{x}} = (\eta_1, \ldots, \eta_n)$. Using this series expansion, the mean of z may be approximated, arriving at the following expression:

$$\eta_z = E[z] = E[h(\mathbf{x})] = \int \ldots \int_{-\infty}^{\infty} h(\mathbf{x}) f_x(\mathbf{x}) = \int \ldots \int_{-\infty}^{\infty} f_x(\mathbf{x}) \left[h(\eta_{\mathbf{x}}) + \sum_{j=1}^{\infty} \sum_{i=1}^{n} \frac{1}{j!} \frac{\partial^j h}{\partial x_i^j} (x_i - \eta_i)^j \right] d\mathbf{x}$$

since

$$\int \ldots \int_{-\infty}^{\infty} (x_{k1} - \eta_{k1})^j \ldots (x_{kl} - \eta_{kl})^q f_x(\mathbf{x}) d\mathbf{x} = 0$$

for every $q, \ldots, j$, if $\exists\ km \neq kn\ m, n \in \{1 \ldots l\}$. Then

$$\eta_z = h(\eta_{\mathbf{x}}) + \sum_{j=2}^{\infty} \sum_{i=1}^{n} \frac{1}{j!} \frac{\partial^j h}{\partial x_i^j} \mu_{j,i} \tag{54}$$

since $\int_{-\infty}^{\infty} (x_k - \eta_k) f_k(x_k) dx_x = 0\ \forall k$.

If we want to approximate the mean η_z by

$$\eta_z \cong \sum_{i=1}^{n} \sum_{k=1}^{m} p_{k,i} h(\eta_1, \ldots, x_{k,i}, \ldots, \eta_n) \tag{55}$$

from the series expansion of the terms of (55) and its aproximation to the series (54) in a similar fashion to the univariate case, equalling terms, we arrive at the following system of equations:

$$\sum_{i=1}^{m} p_{k,i}\xi_{k,i}^{j} = \lambda_{k,j} \tag{56}$$

for $j = 1, \ldots, 2m-1$ and $k = 1, \ldots, n$. For $m = 2$ these equations take the following form for the variable k.

$$\begin{aligned} p_{k,1}\xi_{k,1} + p_{k,1}\xi_{k,1} &= 0 \\ p_{k,1}\xi_{k,1}^{2} + p_{k,2}\xi_{k,2}^{2} &= 1 \\ p_{k,1}\xi_{k,1}^{3} + p_{k,2}\xi_{k,3}^{2} &= \lambda_{k,3} \end{aligned} \tag{57}$$

To these equations, it can be added, for each variable k, that

$$\sum_{i=1}^{m} p_{k,i} = \frac{1}{n} \tag{58}$$

Therefore, there are $2m$ equations with $2m$ unknowns for each variable k, forming a nonlinear system. If $m = 2$, the solution of this system is:

$$\begin{aligned} \xi_{k,i} &= \frac{\lambda_{k,3}}{2} + (-1)^{(3-i)}\sqrt{n + \left(\frac{\lambda_{k,3}}{2}\right)^{2}} \\ p_{k,i} &= \frac{1}{n}(-1)^{j}\frac{\xi_{k,3-i}}{\zeta_k} \end{aligned} \tag{59}$$

where $\zeta_k = 2\sqrt{n + \left(\frac{\lambda_{k,3}}{2}\right)^{2}}$, for $i = 1, 2$, and $k = 1, \ldots, n$.

if $m = 3$, but one of the chosen points if the mean $\eta_{\mathbf{x}}$, only the first four moments of each variable can be fitted. The solution, in this case, is, for each variable k,

$$\begin{aligned} \xi_{k,i} &= \frac{\lambda_{k,3}}{2} + (-1)^{(3-i)}\sqrt{n + \left(\frac{\lambda_{k,3}}{2}\right)^{2}} \\ \xi_{k,3} &= 0 \\ p_{k,i} &= (-1)^{(3-i)}\frac{1}{\xi_{k,i}(\xi_{k,1} - \xi_{k,2})} \\ p_{k,3} &= \frac{1}{n} - p_{k,1} - p_{k,2} = \frac{1}{n} - \frac{1}{\lambda_{k,4} - \lambda_{k,3}^{2}} \end{aligned} \tag{60}$$

for $i = 1, 2$, and $k = 1, \ldots, n$. Since m of the $3m$ point concentrations are in the point η_x, with a weight $p0$, with value

$$p0 = \sum_{k=1}^{n} p_{k,3} = 1 - \sum_{k=1}^{n} \frac{1}{\lambda_{k,4} - \lambda_{k,3}^{2}}$$

this $3m$ concentration scheme can be viewed as a $2m+1$ concentration scheme. The moment of order j of the variable z,$m_{z,j}$, can be then approximated by (61) for the case $2m + 1$.

$$m_{z,j} = E[z^{j}] \cong p0h^{j}(\eta_{\mathbf{x}}) + \sum_{k=1}^{n}\sum_{i=1}^{m} p_{k,i}h^{j}(\eta_1, \ldots, x_{k,i}, \ldots, \eta_n) \tag{61}$$

and in general,

$$m_{z,j} = E[z^j] \cong \sum_{k=1}^{n}\sum_{i=1}^{m} p_{k,i} h^j(\eta_1, \ldots, x_{k,i}, \ldots, \eta_n) \tag{62}$$

The proposed point concentration method should be interpreted as a weighting method rather than a method that discretizes probability distributions. This interpretation must be emphasized since the proposed point estimate method is not a probability distribution transformation method, and the obtained concentrations $p_{k,j}$, $j = 1, \ldots, 2m-1$, and $k = 1, \ldots, n$, are not always nonnegative.

Variable z with low dependance on a variable x_i It must be remarked that when the dependence of the variable z with respect to a variable x_i is very low, or null, the results are similar to consider that this power injection is fixed. For instance, let us consider the case of two random variables, x_1 and x_2. Then, the mean of $z = h(x_1, x_2)$, η_z, if we consider the two variables, must be approximated by

$$\eta_z = p0_{12} h(\eta_1, \eta_2) + p_{1,1} h(x_{11}, \eta_2) + p_{1,2} h(x_{12}, \eta_2) + p_{2,1} h(\eta_1, x_{21}) + p_{2,2} h(\eta_1, x_{22})$$

where $p0_{12}$ is the value of $p0$, considering the two variables x_1 and x_2. If z does not depend on x_1, $h(x_{11}, \eta_2) = h(x_{12}, \eta_2) = h(\eta_1, \eta_2)$. Then,

$$\begin{aligned} \eta_z &= h(\eta_1, \eta_2)(p0_{12} + p_{1,1} + p_{1,2}) + p_{2,1} h(\eta_1, x_{21}) + p_{2,2} h(\eta_1, x_{22}) \\ &= p0_2 h(\eta_1, \eta_2) + p_{2,1} h(\eta_1, x_{21}) + p_{2,2} h(\eta_1, x_{22}) \end{aligned}$$

and $p0_2$ is the value of $p0$, when only the variable x_2 is considered in the system.

Number of equations and unknowns The number of unknowns in the point estimate method, when the $\mathbf{x}$ variables are independents are, for m points (different from the mean) and n variables,

$$NU = 2mn$$

The number of equations that we have, when we make equal the q first moments are qn, and the n equations of the type (58). Therefore, the total number of equations are:

$$NE = n(q+1)$$

Then, equalling these two numbers, we obtain that the order of the needed moment is $q = 2m - 1$.

5.1.2 Dependent random variables.

When the random variable z depends on a set on dependent random variables $\mathbf{x}$, the Taylor series developement of $h(\mathbf{x})$ must take into account the partial derivatives $\frac{\partial^{(kn)} f_x}{\partial x_{k1} \ldots \partial x_{kn}}$, and the formulation becomes more complex. In order to give a view of this added complexity, the analysis of this section will be limited to two variables and the third first central moments.

For these conditions, the series expansion for $\eta_z$is given by

$$\begin{aligned} \eta_z &= h(\eta_1, \eta_2) + \frac{1}{2!}\frac{\partial^2 h}{\partial x_1^2}\mu_{20} + \frac{1}{2!}\frac{\partial^2 h}{\partial x_1 \partial x_2}\mu_{11} + \frac{1}{2!}\frac{\partial^2 h}{\partial x_2^2}\mu_{02} + \\ &\quad \frac{1}{3!}\frac{\partial^3 h}{\partial x_1^3}\mu_{30} + \frac{1}{3!}\frac{\partial^3 h}{\partial x_1^2 \partial x_2}\mu_{21} + \frac{1}{3!}\frac{\partial^3 h}{\partial x_1 \partial x_2^2}\mu_{12} + \frac{1}{3!}\frac{\partial^3 h}{\partial x_2^3}\mu_{03} + \ldots \end{aligned} \tag{63}$$

since, for making an approach of the first third moments, it is necessary to use 10 equations, it is also necessary to have 10 unknowns. If 2 points are considered for each variable, we only have 8 unknowns. Therefore, we need two more, k_1 and k_2 in order to get an approximation of the mean η_z in the following way

$$\eta_z \cong p_{11}h(x_{11},\eta_2) + p_{12}h(x_{12},\eta_2) + k_1 h(x_{11},x_{21}) + k_2 h(x_{12},x_{22}) + p_{21}h(\eta_1,x_{21}) + p_{22}h(\eta_1,x_{22})$$

The series expansion of these terms are shown below

$$\begin{aligned}
h(x_{11},\eta_2) &= h(\eta_1,\eta_2) + \frac{\partial h}{\partial x_1}\xi_{11}\sigma_1 + \frac{1}{2!}\frac{\partial^2 h}{\partial x_1^2}(\xi_{11}\sigma_1)^2 + \frac{1}{3!}\frac{\partial^3 h}{\partial x_1^3}(\xi_{11}\sigma_1)^3 + \dots \\
h(x_{12},\eta_2) &= h(\eta_1,\eta_2) + \frac{\partial h}{\partial x_1}\xi_{12}\sigma_1 + \frac{1}{2!}\frac{\partial^2 h}{\partial x_1^2}(\xi_{12}\sigma_1)^2 + \frac{1}{3!}\frac{\partial^3 h}{\partial x_1^3}(\xi_{12}\sigma_1)^3 + \dots \\
h(x_{11},x_{21}) &= h(\eta_1,\eta_2) + \frac{\partial h}{\partial x_1}\xi_{11}\sigma_1 + \frac{\partial h}{\partial x_2}\xi_{21}\sigma_2 + \\
&\quad \frac{1}{2!}\frac{\partial^2 h}{\partial x_1^2}(\xi_{11}\sigma_1)^2 + \frac{1}{2!}\frac{\partial^2 h}{\partial x_1 \partial x_2}\xi_{11}\sigma_1\xi_{21}\sigma_2\frac{1}{2!}\frac{\partial^2 h}{\partial x_2^2}(\xi_{21}\sigma_2)^2 + \\
&\quad \frac{1}{3!}\frac{\partial^3 h}{\partial x_1^3}(\xi_{11}\sigma_1)^3 + \frac{1}{3!}\frac{\partial^3 h}{\partial x_1^2 \partial x_2}(\xi_{11}\sigma_1)^2\xi_{21}\sigma_2\frac{1}{3!}\frac{\partial^3 h}{\partial x_1 \partial x_2^2}\xi_{11}\sigma_1(\xi_{21}\sigma_2)^2\frac{1}{3!}\frac{\partial^3 h}{\partial x_2^3}(\xi_{21}\sigma_2)^3 + \dots \\
h(x_{12},x_{22}) &= h(\eta_1,\eta_2) + \frac{\partial h}{\partial x_1}\xi_{12}\sigma_1 + \frac{\partial h}{\partial x_2}\xi_{22}\sigma_2 + \\
&\quad \frac{1}{2!}\frac{\partial^2 h}{\partial x_1^2}(\xi_{12}\sigma_1)^2 + \frac{1}{2!}\frac{\partial^2 h}{\partial x_1 \partial x_2}\xi_{12}\sigma_1\xi_{22}\sigma_2\frac{1}{2!}\frac{\partial^2 h}{\partial x_2^2}(\xi_{22}\sigma_2)^2 + \\
&\quad \frac{1}{3!}\frac{\partial^3 h}{\partial x_1^3}(\xi_{12}\sigma_1)^3 + \frac{1}{3!}\frac{\partial^3 h}{\partial x_1^2 \partial x_2}(\xi_{12}\sigma_1)^2\xi_{22}\sigma_2\frac{1}{3!}\frac{\partial^3 h}{\partial x_1 \partial x_2^2}\xi_{12}\sigma_1(\xi_{22}\sigma_2)^2\frac{1}{3!}\frac{\partial^3 h}{\partial x_2^3}(\xi_{22}\sigma_2)^3 + \dots \\
h(\eta_1,x_{21}) &= h(\eta_1,\eta_2) + \frac{\partial h}{\partial x_2}\xi_{21}\sigma_2 + \frac{1}{2!}\frac{\partial^2 h}{\partial x_1^2}(\xi_{21}\sigma_2)^2 + \frac{1}{3!}\frac{\partial^3 h}{\partial x_1^3}(\xi_{21}\sigma_2)^3 + \dots \\
h(\eta_1,x_{22}) &= h(\eta_1,\eta_2) + \frac{\partial h}{\partial x_2}\xi_{22}\sigma_2 + \frac{1}{2!}\frac{\partial^2 h}{\partial x_2^2}(\xi_{22}\sigma_2)^2 + \frac{1}{3!}\frac{\partial^3 h}{\partial x_2^3}(\xi_{22}\sigma_2)^3 + \dots
\end{aligned}$$

Equalling these terms to the moments of equation (63), we arrive at the following system of nonlinear equations

$$\begin{aligned}
p_{11}+p_{12}+k_1+k_2+p_{21}+p_{22} &= 1 \\
(p_{11}+k_1)\xi_{11} + (p_{12}+k_2)\xi_{12} &= 0 \\
(k_1+p_{11})\xi_{21} + (k_2+p_{12})\xi_{22} &= 0 \\
(p_{11}+k_1)\xi_{11}^2 + (p_{12}+k_2)\xi_{12}^2 &= 1 \\
(k_1+p_{21})\xi_{21}^2 + (k_2+p_{22})\xi_{22}^2 &= 1 \\
k_1\xi_{11}\xi_{21} + k_2\xi_{12}\xi_{22} &= \rho \\
(p_{11}+k_1)\xi_{11}^3 + (p_{12}+k_2)\xi_{12}^3 &= \lambda_{1,3} \\
(k_1+p_{21})\xi_{21}^3 + (k_2+p_{22})\xi_{22}^3 &= \lambda_{2,3} \\
k_1\xi_{11}^2\xi_{21} + k_2\xi_{12}^2\xi_{22} &= \frac{\mu_{21}}{\sigma_1^2\sigma_2} \\
k_1\xi_{11}\xi_{21}^2 + k_2\xi_{12}\xi_{22}^2 &= \frac{\mu_{12}}{\sigma_1\sigma_2^2}
\end{aligned} \tag{64}$$

This system can be solved numerically using the Newton-Raphson method. The equations of the error functions and the jacobian matrix can be found in Appendix C.

If moments of higher order, and more variables must be considered, then the number of unknowns and equations changes. The number of moments of order q, when n variables are correlated is the number of combinations with repetition of n variables taken in q, that is to say,

$$CR_q^n = \left(\begin{array}{c} n+q-1 \\ q \end{array} \right) = \frac{(n+q-1)!}{q!(n-1)!}$$

This gives the number of equations to be considered, namely,

$$NE = 1 + \sum_{q=1}^{Q} \left(\begin{array}{c} n+q-1 \\ q \end{array} \right)$$

where Q is the maximum order of the moments considered.

The number of unknowns depends on the number of points to be considered, and the number of variables. It is given, when one of the points is the vector of the mean values, by:

$$NU = 2(m+1)n$$

where m is the number of points (excluded the vector of the means), and n the number of the variables considered. Therefore, it is not always possible to match the number of unknowns and equations, and some additional unknowns must be added, as in the case above, when necessary. A table with the values for several numbers of points, order of moments and number of variables are given below.

Number of moments	No. of variables(n)				
Q	2	3	4	5	6
1	3	4	5	6	7
2	6	10	15	21	28
3	10	20	35	56	84
4	15	35	70	126	210
5	21	56	126	252	462

Table 2: Number of equations

Number of points	No. of variables(n)				
m	2	3	4	5	6
2	10	15	20	25	30
3	14	21	28	35	42
4	18	27	36	45	54
5	22	33	44	55	66
6	26	39	52	65	78
7	30	45	60	75	90
8	34	51	68	85	102
9	38	57	76	95	114

Table 3: Number of unknowns

5.1.3 Computational procedure.

The Point Estimate method can be applied to the Probabilistic load flow to find the uncertainty of the branch power flows and node voltages in the following way [1]:

1. Evaluate the moments of the power injections of each random power source.
2. Solve the system equations (57) and (58). For $m = 2$ and for the $2m + 1$ systems, these solutions are given by (59) and (60), respectively.
3. From these values, run deterministic power flows for the different values of $(\eta_1, \ldots, x_{k,i}, \ldots, \eta_n)$. The solution provides an ensemble of values for the branch power flows and node voltages.

[1] Only for independent random variables.

4. From this ensemble of values, the moments of these variables are found using the equation (61) (or in general (62)).

5. Once the moments found, however, it is still necessary to obtain the values of the PDF or the CDF for the variables of interest. This can be made, for instance, through Gram Charlier or Cornish-Fisher series expansion.

5.2 Computational procedure of ELM.

The ensemble of methods described here make use of the properties of linear combinations of random variables. The theoretical background is given in section 2, and therefore, it will not be repeated here. This section is devoted, thus, to the practical implementation of the method and to show the choice of equations used in it. It must be remarked that the method obtains, at first, the moments of the system variables of interest, and them the values of the CDF at different points.

The methods presented here go from the simplest one, to more general procedures. First, it will be considered only independent random variables, and the DC load flow equations will be used, with a single slack bus. Then, a more general method that considers continuous dependent random variables, and make use of the linear approximation of load flow equations with a distributed slack bus will follow. The most general case presented here considers discrete and dependent continuous variables an uses also linearized AC load flow equations. To obtain a greater accuracy, a Point Estimate method has been used to approximate the mean, while higher order moments are found, as explained, making use of the properties of linear combinations of random variables.

From these values, an estimation of the CDF must be made in all cases. For this, the Cornish-Fisher expansion series is used, and convolutions, whenever the presence of discrete variables make it necessary.

5.2.1 Independent random variables. DC load flow equations. (ELM-IDC)

The proposed method begins from a deterministic evaluation of line flows, using wind power predictions, that will be considered independent random variables. Then, the probabilistic load flow follows, which provides the CDF of the lines of interest. It must be remarked that the deterministic prediction is the expected value of the PDF of the predicted power. Hence, the following steps should be followed to find the CDF of the line flows.

1. Solve a DC load flow with the expected value of the wind power injected to the system. This gives the mean (expected value) of line power flows PDF.

2. Calculate the cumulants of the CDF of the wind power injections, using (3) and (15).

3. Use equation (32) to find the cumulants of the PDF of the power flows through the lines of interest. Coefficients a_{ij} are obtained from equation (44).

4. Use the Cornish-Fisher expansion (41) to find the value of the CDF of the power in the lines of interest.

5.2.2 Dependent continuous random variables. Linearized AC load flow equations (ELM-C).

In this section it is assumed that the random variables are dependent and continuous. The proposed method calculates the CDF of the line flows from the PDF of the power injections through a linear approximation of the load flow equations, taking into account the dependence among the power injections, who are random variables with continuous distributions. It is assumed that there is a forecast of wind power, as well as of load, and a generation scheduling. These set of data will be considered as the base case, around which the linearization is made. The values forecasted are considered to be the mean values of the uncertain power injections. After having modeled the uncertainty of the power injections, it is necessary to calculate the PDF of the line power flows. This is made in two ways: the mean of the distribution is estimated using a point estimate method, without considering the dependence among

variables, while the higher order moments are obtained through the linearization of power flow equations, to take the dependence among variables more easily into account.

The procedure is shown in Figure 15 and explained in the following sections. In this figure r_{max} is the number of lines of interest, and the dotted lines represent the evaluation process, that compares the analytical results to Monte Carlo simulations.

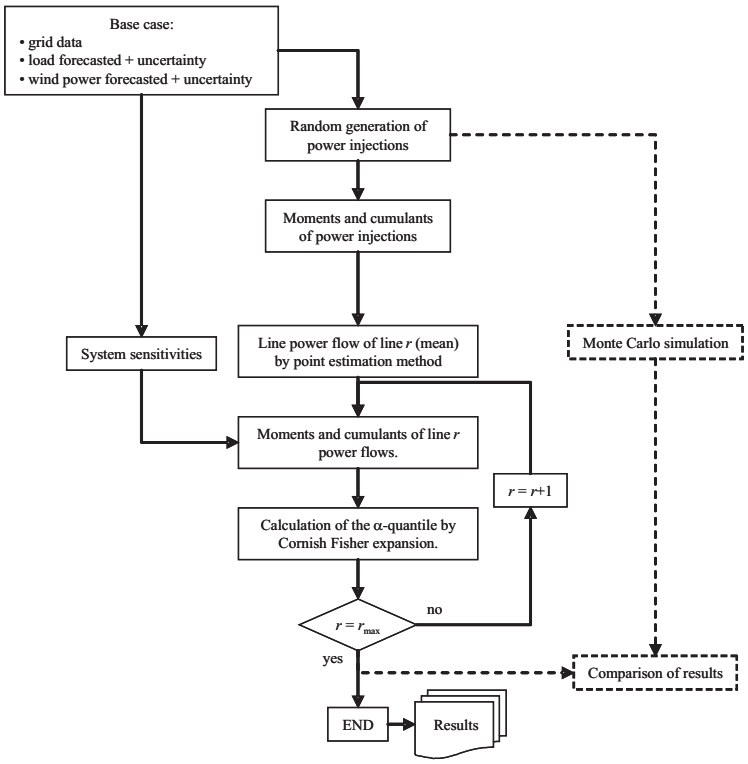

Figure 15: Computational procedure of the proposed method. Dependent continuous random variables.

Base case. The needed data are the grid data, the wind power and load forecasts for the time of interest and the conventional generation scheduling. This is the case that would give the state of the system in a deterministic approach. It is in this base case that the sensitivities described in section 4.2 are calculated.

Uncertainty of power injections. Two kinds of uncertainties are considered in this paper: uncertainty coming from wind power predictions, and load forecast uncertainty. These uncertainties are modeled through their PDF and the dependence among the different power injections are also considered by means of the correlation between random variables. The PDF of the wind power uncertainties considered are modeled as described in section 3.2, taking into account the dependence between the uncertainties. The load uncertainty is modeled as a normal distribution whose mean is the forecasted value. Correlation between load uncertainties has also been considered.

Estimation of the mean values. The line flows in the base case could be taken as an approximation of the mean values of the line flows distributions. However, due to the nonlinearity of the load flow equations, and in order to have a better approximation to the real values, a $(2m + 1)$ point estimate method [4] is used for finding the mean of the line distribution. For this estimation, the dependence among uncertainties is not considered. It has been checked (as shown in the numerical results), that the accuracy is very high for the mean (not for the variance and higher moments) even with this simplification.

Linearization. Calculation of higher order moments of the line flows. The second and higher order moments of the line flows are found using the sensitivity coefficients defined in section 3, by means of the equations provided in section 2.3.6. In order to have a good approximation of the line flows CDF, up to the 5th order moments of the power injections are taken.

Cornish-Fisher expansion. After having found the moments of the distribution of the line flows, a Cornish-Fisher expansion is applied to find the CDF, as explained in section 2.5.2. This allows to find the 90% quantile, for instance, of the line flows, and therefore to check that the probability of surpassing the flow limit is low enough.

5.2.3 Dependent continuous and discrete random variables. Linearized AC load flow equations (ELM).

When discrete variables are considered, the process changes. While the moments are obtained in an identical way, the building of the CDF must be made taking into account the possible multimodal distributions and therefore some convolutions could be made. A flowchart of the method is given in Figure 16.

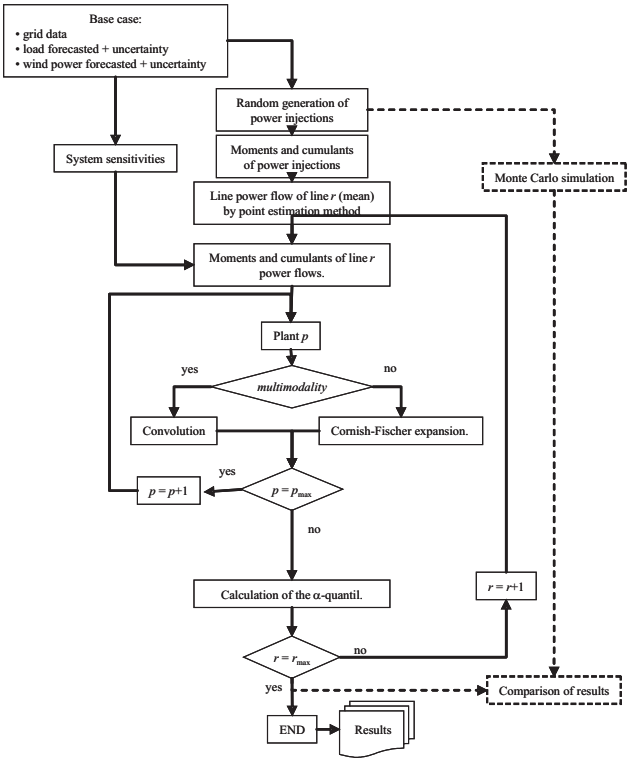

Figure 16: Computational procedure of the proposed method with convolution for discrete and dependent continuous variables.

Base case. It is necessary to have the grid data, the forecasted load and wind power and the scheduled power of the power plant. For this case, the sensitivities of the line power flows to power injections are calculated.

Uncertainty of power injections. These uncertainties are modelled in the following way. Wind power uncertainties are modeled as correlated beta functions whose mean is the forecasted power, and whose variance is estimated as shown in section 3.2. Load uncertainty is modelled as a normal variable

with a given variance. Loads can be dependent or independent. Power plant uncertainties are modelled as binomial variables, as in [30]. Random numbers with the mentioned distributions are generated, taking into account the correlation between variables, as shown in section 2.4.

Calculation of the moments of input variables and mixed moments. There is little or no information about the moments (specially of higher order) of the uncertainty distributions. For this reason, the method used here is to calculate them numerically, using equation (19) from a sample of random numbers of a given PDF. These numbers are generated as described in section 2.4 . They are also used for the Monte Carlo simulation process that has been run to evaluate the accuracy of the results.

Estimation of mean values. The mean values of the line flows are estimated using a $(2m + 1)$ point estimate method, without considering the correlation between random variables. In spite of these simplification, the accuracy of the approximation is very good, as will be shown later.

Higher order moments. Moments of order 2 and higher are calculated using the sensitivity coefficients, by means of the equations provided in section 2.3.6, irrespectively of the continuous or discrete character of the random variables. The moments up to the 5th order are obtained, since they are needed for an accuarate enough Cornish-Fisher expansion, as shown in equation (41).

Building the CDF of branch flows. In this case, discrete and continuous random variables are dealt with in a different way. The process has three steps.

First, the CDF of the branch flows, without considering the discrete variables are estimated using Cornish-Fisher expansion series.

Then, the multimodality condition shown in equation (42) is checked for each line of interest and for each power plant.

If the resulting CDF is not multimodal, then, a simple Cornish-Fisher expansion series is used to approximate the CDF.

If the CDF is multimodal, then the necessary convolutions are made in order to obtain the estimation of the CDF. This process is made at the end, in order to minimize the number of necessary convolutions.

In this way, an approximation of the 90 % quantile (for instance) of the power flow may be obtained, in order to assess the probability of a branch overloading.

In this approach, the moments up to the 5th order have been considered. An easier and reasonable approximation is to consider only up to the second order moments. It will be seen that this alternative approach renders good results, especially in great networks, where conditions are closer to those required by the central limit theorem.

6 Study cases.

In order to show the possibilities of the proposed methods and to quantify their accuracy, a simulation study has been made for different test grids. The chosen grids have been based on the IEEE-RTS grid [21] and the IEEE-118 nodes grid [29], which have been slightly modified to include wind generation.

6.1 Independent wind power productions. DC load flow equations (ELM-DC).

This example is aimed at showing the better approximation properties of the Cornish-Fisher expansion series when compared to Gram-Charlier A series. for this example only continuous independent random variables will be considered, and the DC load flow equations will be used. This does not affect the main conclusions of this study case. The case have been taken from [20].

6.1.1 Network IEEE-RTS

The IEEE-RTS96 system [21] has been modified to include two wind farms. The grid, with the changes from the original system, is shown in Figure 17. The wind farms may represent, in reality, groups of wind farms connected to the transmission network. In the figure, both the rated power (P_n) and the predicted power for a certain moment (P) are written. The lines of interest, where the PDF of the power flows are to be found are the lines 17-16 and 17-22, marked in the same figure. The predicted powers are 300 and 200 MW, which are the expected values of the PDF of the injected power. Since the power ranges of the predictions are low with respect to the wind farm nominal values, the PDF of the injected powers have been modeled as gamma functions. The frequency distribution for a Monte Carlo sampling of 1000 samples, are shown in Figure 18 and in Figure 19. Power base is 100 MW. The two random variables are considered independent.

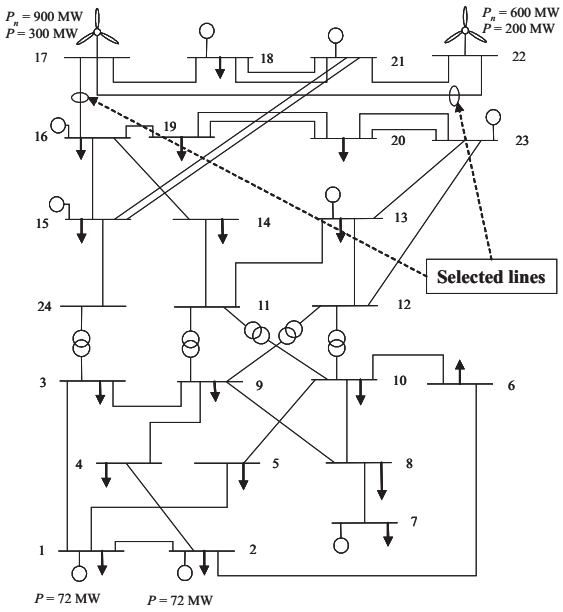

Figure 17: IEEE-RTS96 System with wind farms connected.

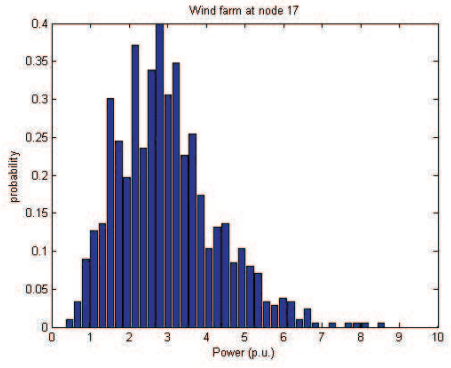

Figure 18: PDF of the power injected by the wind farm connected to node 17.

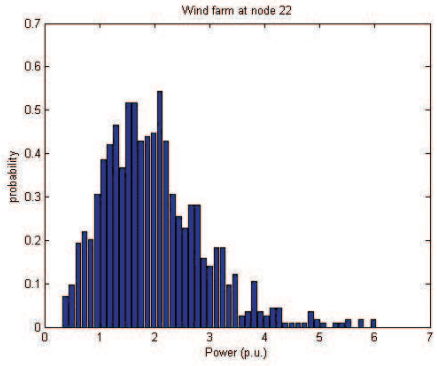

Figure 19: PDF of the power injected by the wind farm connected to node 22.

6.1.2 Results. Comparison between Gram-Charlier A and Cornish-Fisher series.

For this case, the results obtained using the Gram-Charlier series and the Cornish-Fisher expansion are compared to the results from Monte Carlo simulation. Computation times between Gram Charlier and Cornish-Fisher are equivalent, and it has been already demonstrated in other publications, as [22], the smaller computation times of Gram-Charlier series method compared to Monte Carlo simulation, so a comparison of computation times will not be made here. Figure 20 and Figure 21 show the CDF of the lines of interest, using Gram-Charlier expansion series, in comparison with the results using Monte Carlo. It can be seen that the behavior of the Gram-Charlier is poor for both lines.

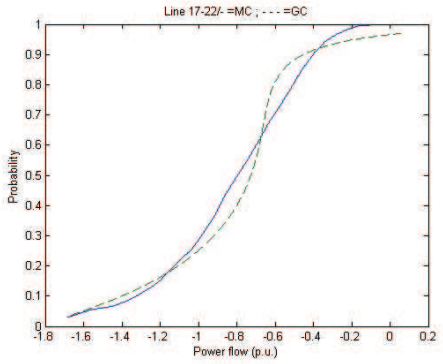

Figure 20: CDF obtained with Monte Carlo simulation and with Gram Charlier expansion series (dotted line). Line 17-22.

Figure 22 and Figure 23 show the CDF for both lines obtained using the Cornish-Fisher expansion, in comparison with the result obtained using Monte Carlo. It can be observed that the fitting in this case is very good.

In order to assess the goodness of the fitness reached by the Cornish-Fisher expansion a Kolmogorov-Smirnov (K-S) test has been made to the results. K-S test [23] is used to determine whether two underlying one-dimensional probability distributions differ, or whether an underlying probability distribution differs from a hypothesized distribution, in either case based on finite samples. In both cases, the K-S test has succeeded, and therefore, the distribution could be considered sufficiently alike to that obtained from Monte Carlo simulation. Results obtained through Gram-Charlier series did not pass this test, as could be expected. Another numerical comparison given here is the difference between the values given by Monte Carlo method and Cornish-Fisher expansion for a quantile of 90%. This is shown in Table 4.

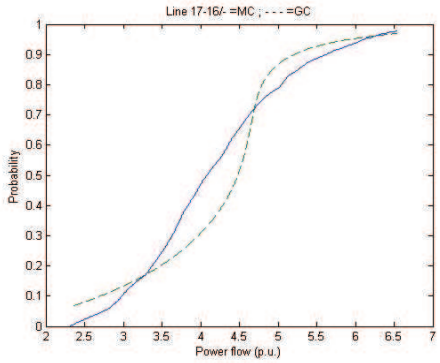

Figure 21: CDF obtained with Monte Carlo simulation and with Gram Charlier expansion series (dotted line). Line 17-16.

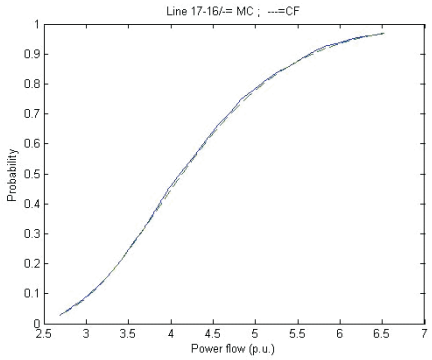

Figure 22: CDF obtained with Monte Carlo simulation and with Cornish-Fisher expansion (dotted line). Line 17-22.

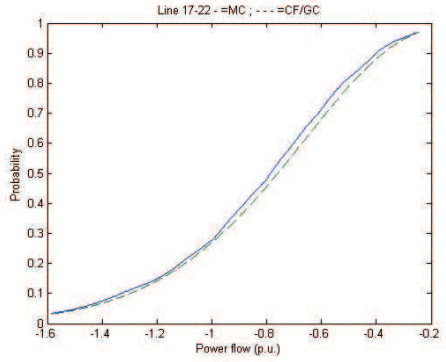

Figure 23: CDF obtained with Monte Carlo simulation and with Cornish-Fisher expansion (dotted line). Line 17-16.

Lines	Absolute error (p.u.)	Relative error (%)
17-22	0.0236	-0.03
17-16	0.0329	0.01

Table 4: Comparison of the results for the 90% values of the lines of interest.

WF	Node	Group	Wind power (MW)	σ(MW)	Rated power (MW)
1	52	1	59.3	25.6	98
2	44	1	31	13.2	51
3	53	1	14.8	6.48	25
4	50	1	8.5	3.66	14
5	84	2	20.1	9.4	36
6	86	2	17	7.2	28
7	83	2	33	15.11	58
8	82	2	50.3	20.84	82
9	2	3	33	14.1	55
10	5	3	20	9.4	36
11	16	3	27	11.2	44
12	13	3	37.5	16.1	62
13	3	3	27	10.5	42
14	14	3	37.5	16.1	62
		TOTAL	416		693

Table 5: Power System Data. Wind Farms included in the the IEEE-118 system.

6.2 Dependent wind power productions (ELM-C).

The method described in section 5.2.2 has been implemented in MATLAB and applied to a grid based on the IEEE-118 nodes case. In this section, the main results of this application are shown. They are compared with the output of a Monte Carlo simulation procedure with 10000 samples, using the AC load flow equations.

This example is aimed at showing the accuracy of the linear approximation, when compared to a point estimate method and Monte Carlo simulation. it intendes also to show the importance of considering the dependence between random continuous variables, that has shown crucial for a reasonable accuracy of results.

6.2.1 Data.

The case considered is the IEEE-118 nodes test system [29], modified to include wind generation with a significant degree of penetration. In order to keep the load level of the system, the wind power has substituted the conventional generation, which has been reduced proportionally. The data of the wind generation are given in Table 5. The standard deviations of the uncertainty distributions are given in column 5. These values have been obtained according to the heuristical rule given in section 3.2.

The wind powers shown are the forecasted production. The wind power installed is 693 MW, for a system load of 3670 MW. The injected wind power in this situation, 416 MW, is the 60% of the rated power. It can be seen from the values of the standard deviation of the random variables, that the actual wind power may differ widely from the forecasted values. In Table 5, the groups of wind farms with dependent production are shown. Wind power predictions of wind farms belonging to different groups are considered independent. The uncertainty of wind farms power predictions is modeled as a multivariate beta function, as described in section 3.2. Correlation coefficients between the wind farms of the same groups are also given. Since there is no documentation available for the dependence between uncertainties of power predictions, realistic correlation coefficients between wind farm power productions has been taken.

	Independent		Dependent	
Moment	ELM-C	P.E.(2m+1)	ELM-C	P.E.(2m+1)
1	0.249	0.197	0.197	0.211
2	1.234	2.751	1.317	28.607
3(*)	29.356	33.208	13.169	78.856
4(*)	1.892	72.472	1.651	79.740
5(*)	21.098	-	12.740	-

(*) selected values

Table 6: Error in % between analytical methods and Monte Carlo simulation.

Group 1

$$\begin{pmatrix} 1 & 0.38 & 0.47 & 0.41 \\ 0.38 & 1 & 0.45 & 0.47 \\ 0.47 & 0.45 & 1 & 0.55 \\ 0.41 & 0.47 & 0.55 & 1 \end{pmatrix}$$

Group 2

$$\begin{pmatrix} 1 & 0.72 & 0.65 & 0.6 \\ 0.72 & 1 & 0.65 & 0.68 \\ 0.65 & 0.65 & 1 & 0.59 \\ 0.6 & 0.68 & 0.59 & 1 \end{pmatrix}$$

Group 3

$$\begin{pmatrix} 1 & 0.35 & 0.46 & 0.23 & 0.32 & 0.21 \\ 0.35 & 1 & 0.28 & 0.33 & 0.19 & 0.22 \\ 0.46 & 0.28 & 1 & 0.25 & 0.15 & 0.17 \\ 0.23 & 0.33 & 0.25 & 1 & 0.19 & 0.21 \\ 0.32 & 0.19 & 0.15 & 0.19 & 1 & 0.22 \\ 0.21 & 0.22 & 0.17 & 0.21 & 0.22 & 1 \end{pmatrix}$$

The active and reactive power of the load buses are modeled as normal distributions, whose mean values equal the base case data, and whose standard deviations are set arbitrarily as follows [22]: 7% from bus 1 to bus 33, 4% from bus 34 to bus 59, 9% from bus 60 to bus 79, and 5% from bus 80 to bus 118. It has been considered that the demand of four nodes (107, 108, 109, 110) is also correlated, being the correlation matrix:

$$\rho_{load} = \begin{pmatrix} 1 & 0.3 & 0.4 & 0.25 \\ 0.3 & 1 & 0.64 & 0.3 \\ 0.4 & 0.64 & 1 & 0.29 \\ 0.25 & 0.3 & 0.29 & 1 \end{pmatrix}$$

6.2.2 Results.

The problem has been solved using two methods, the ELM-C approach proposed here and the Point Estimate method of order $(2m+1)$ without considering dependence between variables, just as proposed in [4] and described in section 5.1. The results show the accuracy of the ELM-C approach, which is similar to the point estimate method in the non-correlated case, and the importance of considering correlation among variables. This dependence does not involve any difficulties with the ELM-C approach, as previously shown. Table 6 includes the average relative difference in % between mean and the central moments of all the lines in the system, with and without considering dependence between variables. Due to the small values of third and higher order in many lines, only those lines whose values are higher than 10^{-6} are considered[2]. This number is an upper limit of the value of the third moment of a Monte Carlo series of values of a normal random variable, i.e., if we generate a Gaussian random sample, the third moment of the series (which should be null) have a value whose upper limit is around 10^{-6}. This will be made in the next study case. The relative error of central moment of order n, ε_n, is defined as:

$$\varepsilon_n = \frac{1}{N_B} \sum_{j=1}^{N_B} \frac{|\mu_{n,j}^{an} - \mu_{n,j}^{MC}|}{|\mu_{n,j}^{MC}|} \cdot 100 \tag{65}$$

Where $\mu_{n,j}^{an}$ is the moment onf order n of branch j found analytically (either with ELM-C or PE), while $\mu_{n,j}^{MC}$ is the same moment obtained by Monte Carlo method. N_B is the number of branches in the grid.

The values in Table 6 show the good accuracy of the approximation of the mean and the variance of both methods, when the variables are independent. The third moment approximation, however, has less

[2]It is better to consider skewness to discriminate small values.

accuracy. However, a bootstrap analysis of the results show that for most lines, the obtained value is within the 95% confidence limit, that is to say that the sparsity of results from the Monte Carlo method is very high. The accuracy of the fourth moment is also higher for the linear approach, even in the independent case. The fifth moment cannot be approximated with the $(2m+1)$ point estimate method. However, when the dependence between variables is considered, the error in the point estimate method becomes higher even for the second moment. This shows the importance of considering correlation for an accurate simulation. In order to show the accuracy of the linear approximation for selected lines, even with this high error of the third moment, the CDF of powers of lines 8-5, 30-38 and 65-68 (those with the highest variations) are shown in Figure 24, together with the result of Monte Carlo simulation.

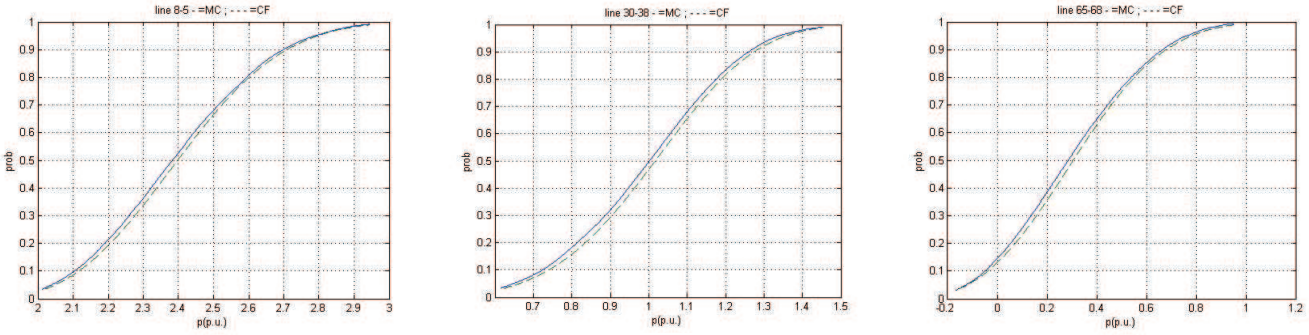

Figure 24: CDFs of selected lines in the IEEE-118 nodes system. MC: Monte Carlo simulation; CF: estimation using Cornish-Fisher expansion.

The relative differences for the 90% quantile are 0.6332%, 1.3370% and 4.4675%. The differences in p.u. are 0.0152 p.u., 0.0136 p.u. and 0.0140 p.u. respectively (absolute value). The average relative error of all the lines of the system is 2.195%. This relative error is defined as

$$\varepsilon_{90} = \frac{1}{N_B} \sum_{j=1}^{N_B} \frac{|p_{90,j}^{ELM} - p_{90,j}^{MC}|}{|p_{90,j}^{MC}|} \cdot 100 \tag{66}$$

Where $p_{90,j}^{ELM}$ and $p_{90,j}^{MC}$ are the 90% quantile of branch j for ELM and the Monte Carlo simulation, respectively.

The program has been run in MATLAB, and the run times of the linear method and the Monte Carlo simulation are 37 s and 443 s respectively, on a processor Intel Pentium of 2.13 GHz with 1 Gb of RAM, for 184 lines in the system.

6.3 Dependent wind power productions with discrete variables (ELM).

In this section, it has been studied the accuray of the linear approach when considering continuous and discrete variables (full ELM) . Results are compared with point estimate method and Monte Carlo simulation.

This method has been applied to two test systems, the IEEE-RTS [21] and the IEEE-118 nodes [29]. The first system is smaller and the AC nonlinearities have a greater effect, specially when the wind penetration is high. In the IEEE-118 system, the conditions are closer to those of the central limit theorem, and the linearity assumption fits also better.

6.3.1 Network IEEE-RTS.

Data. The method has been applied to the IEEE-RTS96 system [21], modified to include wind farms with different generation levels shown in Table 7. The three wind generation scenarios correspond to different productions levels, and have been chosen in order to show the effect of a higher wind power production level. The second scenario is called *normal* because these are the usual levels of wind power

Node	Base case (%)	Normal (%)	High (%)	Rated power (p.u.)
116	51.67	30	80	3
117	50	25	90	6
118	40	24	70	5
122	40	20	85	5

Table 7: Different wind power levels for IEE-RTS case. In % over the rated power.

production of average wind farms. It must be remarked that the shape of the uncertainty PDF changes, as corresponds to the beta distributions (see the Appendix D.1), when the relative production level changes.

The dependence between wind farm powers are given by the following correlation matrix:

$$\rho_{wind} = \begin{pmatrix} 1 & 0.28 & 0.37 & 0.41 \\ 0.28 & 1 & 0.25 & 0.47 \\ 0.37 & 0.25 & 1 & 0.15 \\ 0.41 & 0.47 & 0.15 & 1 \end{pmatrix}$$

Loads have a variance of 5% of the rated load, and the loads of nodes 103, 104, 105 and 108 are also dependent with the following correlation matrix,

$$\rho_{load} = \begin{pmatrix} 1 & 0.3 & 0.4 & 0.25 \\ 0.3 & 1 & 0.64 & 0.3 \\ 0.4 & 0.64 & 1 & 0.29 \\ 0.25 & 0.30 & 0.26 & 1 \end{pmatrix}$$

The availability of power plants has also been considered, and it has been modelled as a binomial variable. Each generation plant is divided into four units with the same power production and a forced outage rate of 0.09, as in [30].

It has also been considered that the plants that compensate load and generation variation are those located in nodes 102, 115 and 123. The changes in generation or load power are equally shared among them.

Results. Probabilistic power flows has been run using Point Estimate $(2m+1)$ method, and the ELM approach described in section 5.2.3. The results are compared with the DC and AC load flow results, to evaluate the effect of system nonlinearities.

The mean values of the linear approach are approximated using the Point Estimate $(2m+1)$ method. The comparison have been made for the three levels of wind production considered. Comparison between moments of active power are summarized in Table 8. This table shows the difference in % between the moments obtained analytically, by the point estimate and the linear approach and those obtained through Monte Carlo simulation. Two cases, AC and DC, have considered for the linear approach. The DC case uses the DC load flow equations for the analytical approach and the Monte Carlo simulation, while the AC case uses the sensitivities obtained in section 4.2, and the results are compared to those of an AC load flow. Again, the error is defined as in equation (65).

The line reactive power flow distributions have been also obtained by the mentioned methods. The mean values of errors for the reactive power are given in Table 9. In this case, only those lines whose variance is higher than 0.05 has been considered. In general, variances and higher order moments of reactive power flows are smaller than those of active power flows. This accounts for one part of the higher values (they are relative values) of the errors associated to these variables. This also reduces the importance of finding the CDF or reactive powers in the system, for the conditions of the problem.

It also interesting to consider the error in the 90% percentile, that is calculated as in equation (66). This value for the branch active powers is summarized in Table 10. In this table, they are shown the average relative errors between the analytical linear approach and the Monte Carlo simulation for all

	Independent			Dependent		
	ELM		P.E.	ELM		P.E.
Moment	DC	AC	$(2m+1)$	DC	AC	$(2m+1)$
Base case						
1	0.95	0.19	0.22	0.46	0.75	0.67
2	0.61	1.98	0.65	0.26	1.54	33.85
3	7.92	32.28	53.71	3.91	39.50	68.34
4	1.84	5.89	67.04	0.61	4.87	77.20
5	11.36	28.76	-	6.46	44.92	-
Normal						
1	0.29	0.14	0.16	0.48	0.23	0.29
2	0.33	3.01	1.09	0.32	3.01	29.43
3	5.04	18.16	21.84	1.14	12.42	52.62
4	1.61	7.88	61.24	0.86	10.03	73.78
5	6.93	21.66	-	2.43	17.78	-
High wind power						
1	0.12	1.65	0.42	1.14	1.28	1.46
2	1.00	2.06	0.82	0.44	3.06	30.06
3	4.58	20.29	18.96	2.25	18.35	56.96
4	1.62	6.53	58.74	1.16	10.94	72.83
5	5.13	25.19	-	2.77	27.03	-

Table 8: Values of ε_n. Continuous and discrete variables. Active power. Grid IEEE-RTS.

	Independent		Dependent	
Moment	ELM	P.E. $(2m+1)$	Linear AC	P.E. $(2m+1)$
Base case				
1	0.25	0.29	3.90	4.33
2	10.55	5.27	15.25	40.40
3	84.38	91.53	82.69	86.37
4	30.36	71.45	35.65	81.34
5	76.71	-	79.67	-
Normal				
1	0.22	0.40	3.92	4.34
2	14.21	1.19	12.61	38.65
3	48.67	35.21	69.65	93.04
4	38.69	62.63	33.91	80.09
5	79.09	-	94.73	-
High wind power				
1	0.24	0.31	2.81	2.49
2	11.60	1.67	14.05	30.73
3	111.45	49.52	102.99	89.10
4	61.98	50.59	79.35	73.69
5	223.34	-	282.52	-

Table 9: Values of ε_n. Continuous and discrete variables. Reactive power. Grid IEEE-RTS.

	Independent				Dependent			
	DC		AC		DC		AC	
	C-F	Normal	C-F	Normal	C-F	Normal	C-F	Normal
Base case								
average (%)	1.96	2.39	1.89	2.37	2.09	2.77	1.88	2.50
max. (p.u.)	0.078	0.148	0.084	0.170	0.109	0.212	0.097	0.198
Normal								
average (%)	1.95	2.73	1.72	2.61	2.12	3.28	1.86	3.20
max. (p.u.)	0.057	0.135	0.058	0.134	0.083	0.210	0.100	0.227
High power								
average (%)	1.67	1.94	1.48	1.72	1.74	2.46	1.38	2.48
max. (p.u.)	0.059	0.140	0.069	0.169	0.070	0.167	0.057	0.162

C-F: Cornish-Fisher expansion; Normal: Normal distribution.

Table 10: Values of ε_{90}. Continuous and discrete variables. Active power. Grid IEEE-RTS.

the lines in the system, and the maximum absolute error, in order to better quantify the quality of the approximation.

In order to show the necessity of considering higher order moments, it has been also calculated the same values when only the mean and variance are considered and assuming that the result follows a normal distribution.

From these results, the following conclusions may be derived. In the independent case, the linear approximation provides results comparable to the point estimate method. The approximation of the second order moment is better with the point estimate method, but the third moment has similar error level, while the fourth order moment is better obtained with the linear approximation. The error in the third moment is quite high due to the sparsity of the values. it has been found that in some lines, with more than a 40% error for this moment, the analytical value is within the 95% confidence interval, when a bootstrap analysis is performed.

With dependent random variables, the results provided by point estimate methods have high errors. It seems, therefore, important to take into account this dependence. The linear approximation yields results accurate enough when dependence is considered. Both with dependent and independent variables, if DC load flow equations are used for the Monte Carlo simulation, the accuracy is very good. System nonlinearities are, as expected, the main source of error.

The accuracy of the linear approximation to moments is high enough to give a good estimation of the probability of a value to be surpassed, as shown in Table 10. In this table, it can also be seen the 90% value of a normal distribution with the same mean and variance. The Cornish-Fisher result yields a higher accuracy, but the normality assumption gives also an useful approximation to the simulated values. This seems to show that, for the giveninput distributions, to consider just the two first moments is enough as a first approach. This will be commented further in the next example.

6.3.2 Network IEEE-118 nodes.

The same method is applied here to a larger network in order to see what happens in more realistic systems. The chosen system is, again, the IEEE-118 nodes network.

Data. The same base case of section 6.2.1 is used here, with some changes. The correlation matrices of wind farms have been changed to:

Branches	Conv.		Analytical	Monte Carlo
28	23		14.52	332,26
172	43	AC	43.98	311.7
		DC	27.23	271.14

Table 11: Computation times, in seconds.

	Independent			Dependent		
	ELM		P.E.	ELM		P.E.
Moment	DC	AC	$(2m+1)$	DC	AC	$(2m+1)$
1	0.31	0.36	0.13	0.35	0.36	0.40
2	0.88	2.00	0.78	0.91	1.82	29.93
3	8.55	13.39	10.07	9.97	12.94	60.56
4	2.24	5.34	59.36	2.72	5.39	77.86
5	11.47	25.97	-	13.65	17.26	-

Table 12: Values of ε_n. Continuous and discrete variables. Active power. Grid IEEE-118

Group 1

$$\begin{pmatrix} 1 & 0.88 & 0.87 & 0.91 \\ 0.88 & 1 & 0.85 & 0.87 \\ 0.87 & 0.85 & 1 & 0.85 \\ 0.91 & 0.87 & 0.85 & 1 \end{pmatrix}$$

Group 2

$$\begin{pmatrix} 1 & 0.82 & 0.85 & 0.9 \\ 0.82 & 1 & 0.85 & 0.88 \\ 0.85 & 0.85 & 1 & 0.89 \\ 0.9 & 0.88 & 0.89 & 1 \end{pmatrix}$$

Group 3

$$\begin{pmatrix} 1 & 0.85 & 0.86 & 0.83 & 0.82 & 0.91 \\ 0.85 & 1 & 0.88 & 0.83 & 0.89 & 0.92 \\ 0.86 & 0.88 & 1 & 0.85 & 0.95 & 0.87 \\ 0.83 & 0.83 & 0.85 & 1 & 0.89 & 0.91 \\ 0.82 & 0.89 & 0.95 & 0.89 & 1 & 0.82 \\ 0.91 & 0.92 & 0.87 & 0.91 & 0.82 & 1 \end{pmatrix}$$

The availability of power plants has also been considered, and it has been modelled as a binomial variable. Each generation plant is divided into four units with the same power production and a forced outage rate of 0.09, as in [30].

It has also been considered that the plants that compensate load and generation variation are those located in nodes 10, 25, 46, 54, 61, 66 and 100. The changes in generation or load power are shared equally among them.

Results. The problem has been solved using two methods: point estimate $(2m+1)$ and the linear approach described in section 5.2.3. In this case the results have been compared to an AC load flow, and also to simulations using DC load flow, to show the influence of nonlinearities of AC equations on the final results.

Computation times depend largely, for the analytical case of the lines of interest and of the number of convolutions performed. Some values are given for the IEEE-118 test system used, under different conditions, in Table 11. They have been obtained with a processor Intel Pentium of 2.13 GHz with 1 Gb of RAM. Roughly, it could be said that the computation times needed are a 10% of those necessary in a Monte Carlo simulation, with 10000 samples.

The accuracy of the approximation of moments is shown in Table 12 for different cases. It must be remembered that the mean in both cases is obtained with the Point Estimate method.

From these results, the following conclusions may be made.

The point estimate method yields a good approximation for the independent case up to the second order moment. Estimation of higher order moment has also higher errors. The method, however, behaves poorly when the input random variables are dependent.

The linear approximation, on the other hand yields worse results for the independent case, although the error remains similar to the point estimate case. For the dependent case, the results have similar accuracy, and they yield satisfactory results.

This is better seen in the comparison between 90% percentile errors given in Table 13.

Normality assumption also gives good results, even better than in the IEEE-RTS system. This higher accuracy may be due to the better compliance with the conditions of the Central Limit Theorem, as there

	Independent				Dependent			
	AC		DC		AC		DC	
	C-F	Normal	C-F	Normal	C-F	Normal	C-F	Normal
average (%)	1.93	2.73	1.95	3.06	1.83	2.03	1.81	2.13
max. (p.u.)	.160	.089	.142	.094	.077	.061	.064	.066

C-F: Cornish-Fisher expansion; Normal: Normal distribution.

Table 13: Values of ε_{90}. Continuous and discrete variables. Active power. Grid IEEE-118

	Independent		Dependent	
Moment	ELM	P.E. $(2m+1)$	ELM	P.E. $(2m+1)$
1	1.01	0.95	2.04	1.80
2	25.41	9.40	22.88	30.36
3	102.24	152.46	97.42	155.48
4	58.45	82.26	45.74	86.84
5	142.33	-	132.12	-

Table 14: Values of ε_n. Continuous and discrete variables. Reactive power. Grid IEEE-118

are more random variables.

The results for the reactive power are given in Table 14. Again, the mean is calculated in both cases with the point estimate method. The results of the point estimate method in the independent case are better than the linear approximation for the second moment, but in the dependent case the linear approximation behaves better than the point estimate method. In all the cases the result is not very good, as could be expected. This is due, not only to the higher nonlinearity of reactive power with respect to input power, but to the smaller variability of this variable. For instance, for the case of linearized AC equation with dependent variables, the average variance of branch active powers is 0.019, while that of reactive powers is $5.73 \cdot 10^{-4}$. The maximum values are 0.4749 and 0.0132. For higher moments, the differences are even larger. The importance of considering reactive power variations is, therefore, smaller.

It is also interesting to compare the CDF and PDF of the Monte Carlo simulation, the result of Cornish-Fisher expansion, and the Normal approximation, i.e., a normal distribution of the same mean and variance. The comparison will be made for three different cases. Firstly, a good aproximation of both Cornish-Fisher expansion and normal distribution are shown in Figures 25 for the CDF and 26 for the PDF. In this case, it can also be seen that the expected variation in the power flow are small, because the influences of the random variables in the line flow are also small.

Figures 27 and 28 show the PDF and the CDF, respectively, of a line where the possible flow are likely to change much more than in the previous case. The normal approximation separates from the Monte Carlo simulation results, while the Cornish-Fisher result fits quite well to the final distribution. Differences are smaller in the CDF, where the normality assumption also yields a small error.

On the other hand, when the influence of a discrete variable (the uncertainty of a power plant production) has a large enough impact on the line power flows, multilinearity appears, as shown in Figures 29 and 29. The normality assumption gives a bad approximation for the PDF, and CDF. In this case, it is necessary to perform a convolution (or more than one) to obtain a good approximation. It must be remarked that the convolutions are only performed whenever they are needed: in the previous cases shown (Figures 25 to 28), no convolution were necessatry and they were not made.

Although the method has been developed also for voltages, the changes in the voltages, with a distributed slack bus are extremely small, and the results are not presented here.

7 Conclusion.

Probabilistic power flows become more important in systems with high wind power penetration, because of the high variability of the input/injected power. When considering daily system operation in systems with high wind penetration, it is necessary to consider the uncertainty of short term wind power prediction.

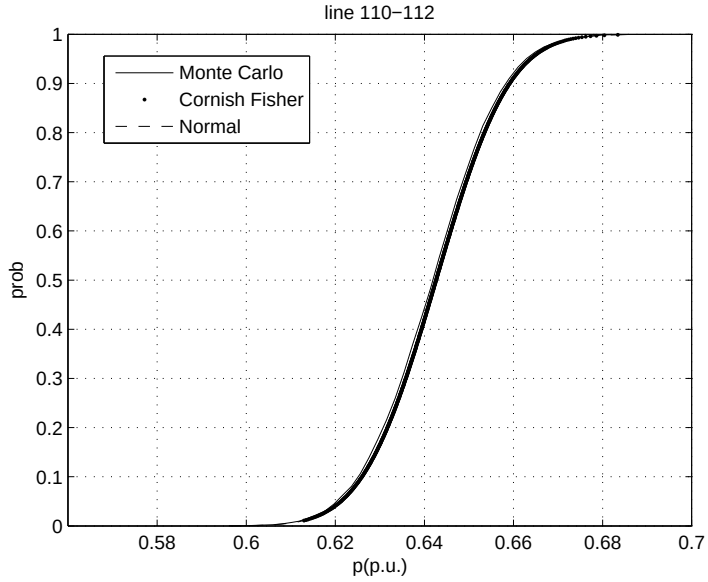

Figure 25: Comparison of CDFs of different methods.

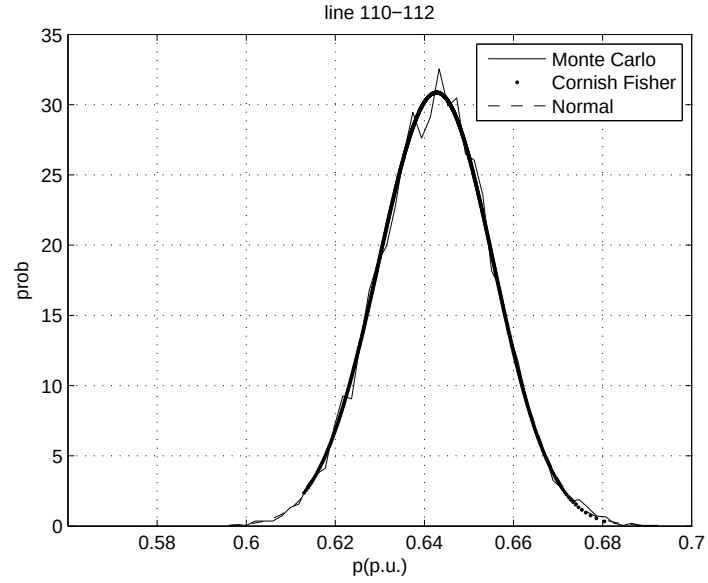

Figure 26: Comparison of PDFs of different methods.

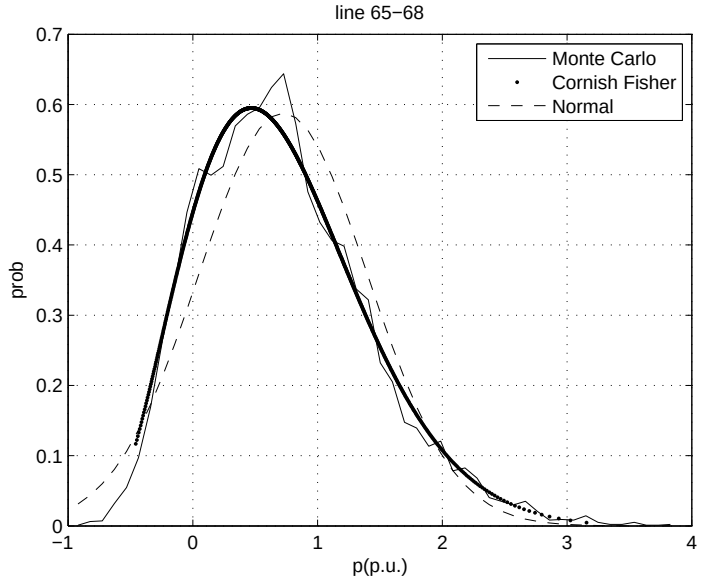

Figure 27: Comparison of PDFs of different methods.

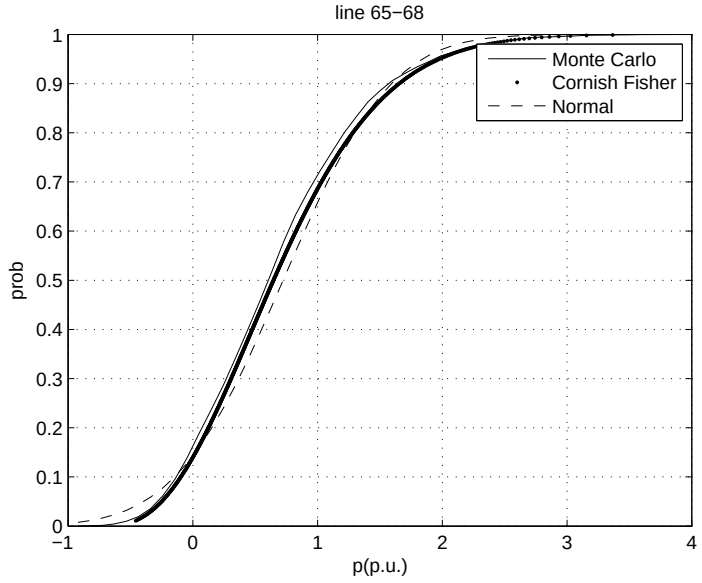

Figure 28: Comparison of CDFs of different methods.

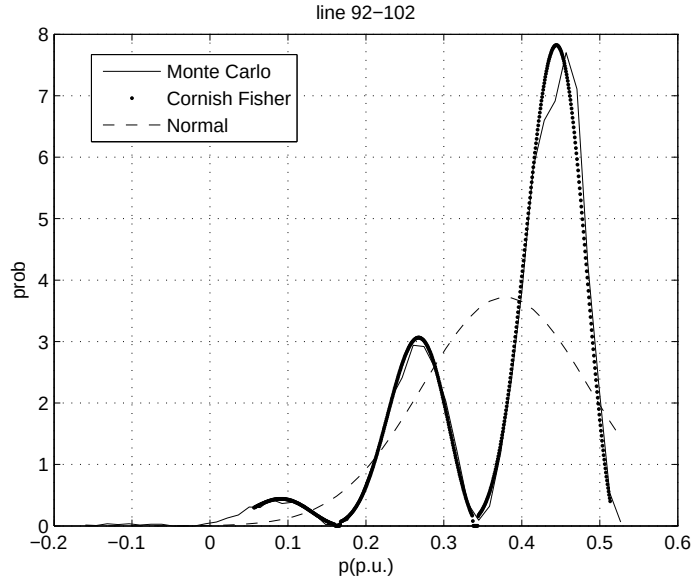

Figure 29: Comparison of CDFs of different methods.

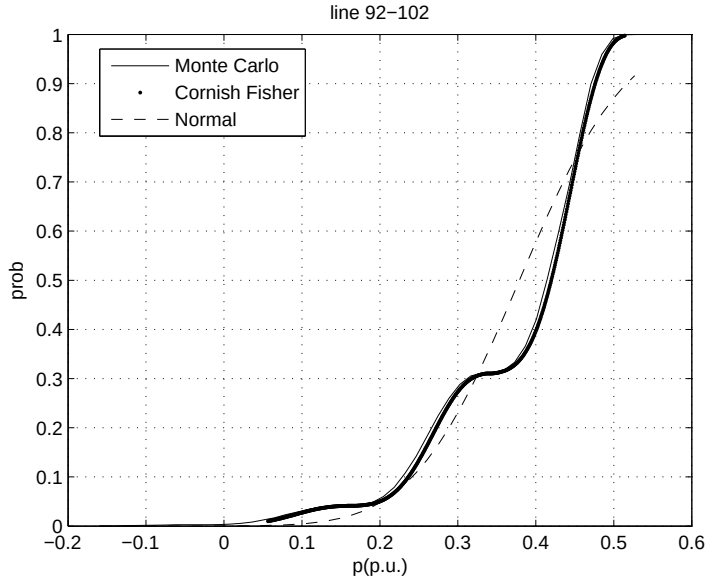

Figure 30: Comparison of CDFs of different methods.

Wind power prediction uncertainty has not been yet exhaustively studied, due to the recent development of forecasting tools, and the limited experience. The PDF that model this uncertainty must be bounded and usually asymmetric, since their shape depends on the power level and on the time horizon of the prediction. In general, they cannot be assumed to be Gaussian, and a Beta distribution is a better choice. The uncertainties of wind power farms within a zone are correlated. This correlation is much smaller when distant zones are considered.

Recent approaches to the proabilistic load flow problem focus on obtaining, at a first stage, the moments of the grid random variables of interest (mainly power flows through lines). Point estimate method is one of these approaches. This method gives good results when the input variables (uncertainties of loads and wind power predictions) are independent. It is however difficult to generalize this formulation for dependent random variables. To neglect this dependence yields sizeable errors, and therefore, their interest is limited, for the considered problem.

Once the moments of the distributions of output variables have been obtained, it is necessary to estimate also the probability of surpassing a limit (maximum power flows, for instance), i.e., it is necessary to estimate the PDF or CDF of the random variable. Recently, series expansion methods, such as Gram-Charlier A series or Cornish-Fisher series have been proposed to solve this problem. Cornish-Fisher expansion series seem to behave better with non-Gaussian functions (such as those of interest in this study). This approximation yields a good fitting for unimodal distributions. Absolute errors are small, and relative errors have also very low values. To approximate the output PDF by a normal distribution yields a reasonable approximation of the higher percentiles, even if the fitting of the resulting PDF to them is poor in the studied cases.

When power plant reliability, or other discrete input random variable are to be considered, some of the PDF of the output variables may be multimodal. This circumstance poses some additional difficulties to the percentile calculation problem. The most obvious way of solving it, assuming independence between the discrete and the continuous variables, is to convolve both variables. This technique is, however, computationally expensive, and it is useful to perform it only when necessary, because not every combination of discrete and continuous random variables yields a multimodal distribution, and therefore it is not necessary to make a convolution. To discriminate between necessary and unnecessary convolutions, an unimodality test can be made in the frequency domain. If convolutions are only made when this test is not passed, the number of necessary convolutions reduces dramatically. Obviously, the normality assumption does not hold for multimodality conditions.

8 Acknowledgment.

This work has been undertook within the research projects Anemos Plus (6th FP European Project. Reference 38692) and IEMEL, Research Project of the Spanish Ministry of Education (Reference ENE2006-05192/ALT).

Most of this work has been made during a sabbatical leave from the Universidad Carlos III de Madrid in Supélec, France. The stay has been also financed by the Spanish Ministry of Education within the program "Estancias de profesores e investigadores españoles en centros de enseñanza superior e investigación extranjeros" (Reference PR2007-0032).

A Relations between moments, central moments and cumulants

A.1 Moments and central moments.

The central moments can be written as a function of moments as shown here,

$$\begin{aligned}
\mu_0 &= 1 \\
\mu_1 &= 0 \\
\mu_2 &= m_2 - m_1^2 \\
\mu_3 &= m_3 - 3m_1m_2 + 2m_1^3 \\
\mu_4 &= m_4 - 4m_1m_3 + 6m_1^2m_2 - 3m_1^4
\end{aligned}$$

and,inversely,

$$\begin{aligned}
m_2 &= \mu_2 + m_1^2 \\
m_3 &= \mu_3 + 3m_1\mu_2 + m_1^3 \\
m_4 &= \mu_4 + 4m_1\mu_3 + 6m_1^2\mu_2 + m_1^4 \\
m_5 &= \mu_5 + 5\mu_4m_1^4 + 10\mu_3m_1^2 + 10\mu_2m_1^3 + m_1^5
\end{aligned}$$

A.2 Central moments and cumulants[11].

Moments as functions of cumulants

$$\begin{aligned}
m_1 &= \kappa_1 \\
m_2 &= \kappa_2 + \kappa_1^2 \\
m_3 &= \kappa_3 + 3\kappa_2\kappa_1 + \kappa_1^2 \\
m_4 &= \kappa_4 + 4\kappa_3\kappa_1 + 3\kappa_2^2 + 6\kappa_2\kappa_1^2 + \kappa_1^4 \\
m_5 &= \kappa_5 + 5\kappa_4\kappa_1 + 10\kappa_3\kappa_2 + 10\kappa_3\kappa_1^2 + 15\kappa_2^2\kappa_1 + 10\kappa_2\kappa_1^3 + \kappa_1^5 \\
m_6 &= \kappa_6 + 6\kappa_5\kappa_1 + 15\kappa_4\kappa_2 + 15\kappa_4\kappa_1^2 + 10\kappa_3^2 + 60\kappa_3\kappa_2\kappa_1 + 20\kappa_3\kappa_1^3 + 15\kappa_2^3 + 45\kappa_2^2\kappa_1^2 + 15\kappa_2\kappa_1^4 + \kappa_1^6
\end{aligned}$$

Central moments as functions of cumulants

$$\begin{aligned}
\mu_2 &= \kappa_2 \\
\mu_3 &= \kappa_3 \\
\mu_4 &= \kappa_4 + 3\kappa_2^2 \\
\mu_5 &= \kappa_5 + 10\kappa_3\kappa_2 \\
\mu_6 &= \kappa_6 + 15\kappa_4\kappa_2 + 10\kappa_3^2 + 15\kappa_2^3
\end{aligned}$$

Cumulants as functions of moments,

$$\begin{aligned}
\kappa_1 &= m_1 \\
\kappa_2 &= m_2 - m_1^2 \\
\kappa_3 &= m_3 - 2m_2m_1 + 2m_1^2 \\
\kappa_4 &= m_4 - 4m_3m_1 - 3m_2^2 + 12m_2m_1^2 - 6m_1^4 \\
\kappa_5 &= m_5 - 5m_4m_1 - 10m_3m_2 + 20m_3m_1^2 + 30m_2^2m_1 - 60m_2m_1^3 + 24m_1^5 \\
\kappa_6 &= m_6 - 6m_5m_1 - 15m_4m_2 + 30m_4m_1^2 - 10m_3^2 + 120m_3m_2m_1 - 120m_3m_1^3 \\
&\quad +30m_2^3 - 270m_2^2m_1^2 + 360m_2m_1^4 - 120m_1^6
\end{aligned}$$

Cumulants as functions of central moments,

$$\begin{aligned}
\kappa_2 &= \mu_2 \\
\kappa_3 &= \mu_3 \\
\kappa_4 &= \mu_4 - 3\mu_2^2 \\
\kappa_5 &= \mu_5 - 10\mu_3\mu_2 \\
\kappa_6 &= \mu_6 - 15\mu_4\mu_2 - 10\mu_3^2 + 30\mu_2^3
\end{aligned}$$

B Tchebycheff-Hermite polynomials.[11]

A distribution $\varphi(x)$ that is N(0,1) can be written as

$$\varphi(x) = \frac{1}{\sqrt{2\pi}} e^{-\frac{1}{2}x^2}$$

If we define

$$D = \frac{d}{dx} \tag{67}$$

the succesive derivatives of $\varphi(x)$ with respect to x are

$$\begin{aligned}
D\varphi(x) &= -x\varphi(x) \\
D^2\varphi(x) &= (x^2 - 1)\varphi(x) \\
D\varphi(x) &= (3x - x^3)\varphi(x)
\end{aligned}$$

The result will be a polynomial in x multiplied by $\varphi(x)$. We then define the Tchebycheff-Hermite polynomial $H_r(x)$ by the identity

$$(-D)^r\varphi(x) = H_r(x)\varphi(x) \tag{68}$$

$H_r(x)$ is of degree r in x and the coefficient of x^r is unity. By convention $H_0 = 1$. The first ten polinomials are:

$$\begin{aligned}
H_0 &= 1 \\
H_1 &= x \\
H_2 &= x^2 - 1 \\
H_3 &= x^3 - 3x \\
H_4 &= x^4 - 6x^2 + 3 \\
H_5 &= x^5 - 10x^3 + 15x \\
H_6 &= x^6 - 15x^4 + 45x^2 - 15 \\
H_7 &= x^7 - 21x^5 + 105x^3 - 105x \\
H_8 &= x^8 - 28x^6 + 210x^4 - 420x^2 + 105 \\
H_9 &= x^9 - 36x^7 + 378x^5 - 1260x^3 + 945x \\
H_{10} &= x^{10} - 45x^8 + 630x^6 - 3150x^4 + 4725x^2 - 945
\end{aligned}$$

to obtain further terms the following recurrence equation can be used

$$H_r(x) = xH_{r-1}(x) - (r-1)H_{r-2}(x)$$

The polynomials have an important orthogonal property, namely, that

$$\left.\begin{array}{rr} \int_{-\infty}^{\infty} H_m(x)H_n(x)\varphi(x)dx = 0, & m \neq n \\ = n! & m = n \end{array}\right\} \tag{69}$$

C Solution by Newton-Raphson of equations (64).

The error functions of (64) are

$$\begin{aligned}
\varepsilon_1 &= p_{11} + p_{12} + k_1 + k_2 + p_{21} + p_{22} - 1 \\
\varepsilon_2 &= (p_{11} + k_1)\xi_{11} + (p_{12} + k_2)\xi_{12} \\
\varepsilon_3 &= (k_1 + p_{11})\xi_{21} + (k_2 + p_{12})\xi_{22} \\
\varepsilon_4 &= (p_{11} + k_1)\xi_{11}^2 + (p_{12} + k_2)\xi_{12}^2 - 1 \\
\varepsilon_5 &= (k_1 + p_{21})\xi_{21}^2 + (k_2 + p_{22})\xi_{22}^2 - 1 \\
\varepsilon_6 &= k_1\xi_{11}\xi_{21} + k_2\xi_{12}\xi_{22} - \rho \\
\varepsilon_7 &= (p_{11} + k_1)\xi_{11}^3 + (p_{12} + k_2)\xi_{12}^3 - \lambda_{1,3} \\
\varepsilon_8 &= (k_1 + p_{21})\xi_{21}^3 + (k_2 + p_{22})\xi_{22}^3 - \lambda_{2,3} \\
\varepsilon_9 &= k_1\xi_{11}^2\xi_{21} + k_2\xi_{12}^2\xi_{22} - \frac{\mu_{21}}{\sigma_1^2\sigma_2} \\
\varepsilon_{10} &= k_1\xi_{11}\xi_{21}^2 + k_2\xi_{12}\xi_{22}^2 - \frac{\mu_{12}}{\sigma_1\sigma_2^2}
\end{aligned} \tag{70}$$

and the jacobian matrix has the following expression

$$J = \begin{bmatrix}
1 & 1 & 1 & 1 & 0 & 0 & 0 & 1 & 1 & 1 \\
\xi_{11} & \xi_{12} & 0 & 0 & (p_{12}+k_1) & (p_{12}+k_2) & 0 & 0 & \xi_{11} & \xi_{12} \\
0 & 0 & \xi_{21} & \xi_{22} & 0 & 0 & (k_1+p_{21}) & (k_2+p_{22}) & \xi_{21} & \xi_{22} \\
\xi_{11}^2 & \xi_{12}^2 & 0 & 0 & 2(p_{11}+k_1)\xi_{11} & (p_{12}+k_2)\xi_{12} & 0 & 0 & \xi_{11}^2 & \xi_{12}^2 \\
0 & 0 & \xi_{21}^2 & \xi_{22}^2 & 0 & 0 & 2(k_1+p_{21})\xi_{21} & 2(k_2+p_{22})\xi_{22} & \xi_{21}^2 & \xi_{22}^2 \\
0 & 0 & 0 & 0 & k_1\xi_{21} & k_2\xi_{22} & k_1\xi_{11} & k_2\xi_{12} & \xi_{11}\xi_{21} & \xi_{12}\xi_{22} \\
\xi_{11}^3 & \xi_{12}^3 & 0 & 0 & 3(p_{11}+k_1)\xi_{11}^2 & 3(p_{12}+k_2)\xi_{12}^2 & 0 & 0 & \xi_{11}^3 & \xi_{12}^3 \\
0 & 0 & \xi_{21}^3 & \xi_{22}^3 & 0 & 0 & 3(k_1+p_{11})\xi_{21}^2 & 3(k_2+p_{22})\xi_{22}^2 & \xi_{21}^3 & \xi_{22}^3 \\
0 & 0 & 0 & 0 & 2k_1\xi_{11}\xi_{21} & 2k_2\xi_{12}\xi_{22} & k_1\xi_{11}^2 & k_2\xi_{12}^2 & \xi_{11}^2\xi_{21} & \xi_{12}^2\xi_{22} \\
0 & 0 & 0 & 0 & k_1\xi_{21}^2 & k_2\xi_{22}^2 & 2k_1\xi_{11}\xi_{21} & 2k_2\xi_{12}\xi_{22} & \xi_{11}\xi_{21}^2 & \xi_{12}\xi_{22}^2
\end{bmatrix}$$

The unknowns are written in the following order

$$\begin{bmatrix} p_{11} & p_{12} & p_{21} & p_{22} & \xi_{11} & \xi_{12} & \xi_{21} & \xi_{22} & k_1 & k_2 \end{bmatrix}^t$$

D Some distributions.

D.1 Beta distribution.

The analytical expression of beta probability density function is

$$f(x;a,b) = \frac{1}{B(a,b)}x^{a-1}(1-x)^{b-1}$$

Where $B(a,b)$ is the beta function, and a and b are parameters related to the mean, η , and the variance, σ^2, in the following way:

$$\eta = \frac{a}{a+b} \qquad \sigma^2 = \frac{ab}{(a+b)^2(a+b+1)}$$

The beta distribution has been represented in Figure 31.

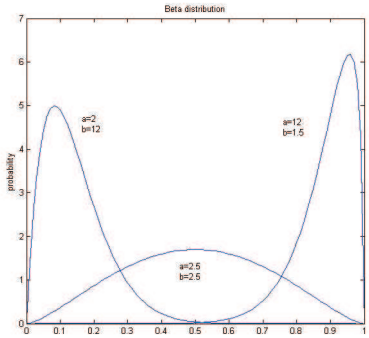

Figure 31: Beta distribution for different values of parameters a and b.

D.2 Binomial distribution.

Binomial distribution is the discrete probability distribution of the number of successes in a sequence of n independent yes/no experiments, each of which yields success with probability p.

In general, if the random variable K follows the binomial distribution with parameters n and p, we write $K \sim B(n, p)$. The probability of getting exactly k successes is given by the probability mass function:

$$f(k; n, p) = \left(\begin{array}{c} n \\ k \end{array} \right) p^k (1-p)^{n-k}$$

The mean of this distribution is $\eta = np$, and the variance is $\sigma^2 = np(1-p)$.

D.3 Exponential distribution.

In probability theory and statistics, the exponential distributions are a class of continuous probability distributions. An exponential distribution arises naturally when modeling the time between independent events that happen at a constant average rate.

The probability density function (pdf) of an exponential distribution has the form:

$$f(x, \lambda) = \left\{ \begin{array}{ccc} \lambda e^{-\lambda x} & , & x \geq 0 \\ 0 & , & x < 0 \end{array} \right.$$

The mean of this distribution is $\eta = \frac{1}{\lambda}$, and the variance is $\sigma^2 = \frac{1}{\lambda^2}$.

References

[1] Borkowska B. "Probabilistic load flow" *IEEE Trans. Power App. Syst.*, vol. PAS-93, pp. 752-759, May 1974.

[2] Dopazo J.F. "Stochastic load flow" *IEEE Trans. Power App. Syst.*, vol. PAS-94, pp. 299-309, March 1975.

[3] Allan R. N., Da Silva A. M. L., Burchett R. C. "Evaluation methods and accuracy in probabilistic load flow solutions," *IEEE Trans. Power App. Syst.*, vol. PAS-100, pp. 2539-2546, May 1981.

[4] Su C-L., "Probabilistic Load-Flow Computation Using Point Estimate Method." *IEEE Trans. on Power Systems*. Vol. 20, No. 4, November 2005.

[5] Hatziargyriou N.D., Karakatsanis T.S., Papadopoulos M., "Probabilistic Load Flow in Distribution Systems Containing Dispersed Wind Power Generation", *IEEE Trans. Power. Sys.*, vol. PWRS-8, pp. 159-165, February 1993

[6] Usaola J. "Probabilistic load flow with wind production uncertainty using cumulants and Cornish-Fisher expansion." *Proceedings of the 2008 PSCC*. Glasgow (UK), July 2008.

[7] Leite da Silva A.M., Arienti V.L., Allan R.N. "Probabilistic Load Flow Considering Dependence Between Input Nodal Powers", *IEEE Trans. Power. App. and Sys.*, vol. PAS-103, pp. 1524-1530, June 1984.

[8] Sanabria L.A., Dillon T.S. "Power system reliability assessment suitable for a deregulated system via the method of cumulants", *Electric Power and Energy Systems*, vol. 20, pp. 203-211, February 1993.

[9] Papoulis A., Pillai S.U. *Probability, Random Variables and Stochastic Processes*. 4th Ed. McGraw-Hill, Boston 2002.

[10] McCullagh P. "Tensor Methods in Statistics". Chapman & Hall. London, 1987.

[11] Kendall M.G., Stuart A. *The Advanced Theory of Statistics. Vol. I.* Charles Griffin & Co. Ltd., London 1958.

[12] Blinnikov S., Moessner R. "Expansions for nearly Gaussian distributions." *Astron. Astrophys. Suppl. Ser.* Vol. 130, pp. 193-205, (1998).

[13] Cornish E.A., Fisher R.A., "Moments and cumulants in the specification of distributions". *Revue de l'Institut Internat. de Statis.* Vol. 4, pp. 307-320 (1937).

[14] Cramér H. *Métodos matemáticos de estadística*. Aguilar, Madrid 1953.

[15] Cramér H. "On some classes of series used in mathematical statistics" *Proceedings of the Sixth Scandinavian Congr. of Math.*, Kobenhavn, 1925.

[16] Hill G.W., Davis A.W. "Generalized asymptotic expansions of Cornish-Fisher type". *The Annals of Mathematical Statistics*. Vol. 39, No. 4, pp.1264-1273. (1968).

[17] Jaschke S.R. "The Cornish-Fisher-Expansion in the Context of Delta-Gamma-Normal Approximations." `http://www.jaschke-net.de/papers/CoFi.pdf`. Discussion Paper 54, Sonderforschungsbereich 373, Humboldt-Universität zu Berlin.

[18] Focken U., Lange M., Moennich K., Waldl H.P., Beyer H.G., Luig A. "Short-term prediction of the aggregated power output of wind farms - a statistical analysis of the reduction of the prediction error by spatial smoothing effects". *Journal of Wind Engineering and Industrial Aerodynamics*. Vol. 90 (2002) pp. 231-246.

[19] Holton G.A. *Value-at-Risk. Theory and Practice*. Academic Press, Elsevier (2004).

[20] J. Usaola "Probabilistic Load Flow with Wind Production Uncertainty using Cumulants and Cornish Fisher Expansion." *Proceedings of the 2008 Power Systems Computation Conference*. Glasgow (UK), July 2008.

[21] "The IEEE Reliability Test System." *IEEE Trans. on Power Systems* Vol. 14, pp. 1010-1018, (1999).

[22] P. Zhang, T. Lee, "Probabilistic Load Flow Computation Using the Method of Combined Cumulants and Gram-Charlier Expansion", *IEEE Trans. Power. Sys.*, Vol. PWRS-19, pp. 676-682, (2004).

[23] G.M Clarke, D. Cooke, *A Basic Course in Statistics*. Arnold, London 1998.

[24] A.C. Miller, T.R. Rice "Discrete approximations of probability distributions". *Management Science*, Vol. 29, pp. 352-363 (1983).

[25] G. Kariniotakis et al. "Evaluation of Advanced Wind Power Forecasting Models -Results of the Anemos Project" *Proceedings of the EWEC*. Athens, 2006.

[26] G. González, B. Díaz-Guerra, F. Soto, S. López, I. Sánchez, J. Usaola, M. Alonso, M.G. Lobo "SIPREÓLICO-Wind power prediction tool for the Spanish peninsular power system." *Proceedings of the CIGRÉ 40th General Session & Exhibition*. París (France), August 2004.

[27] A.Fabbri, T. Gómez San Román, J. Rivier, V.H. Méndez Quezada "Assessment of the Cost Associated With Wind Generation Prediction Errors in a Liberalized Electricity Market." *IEEE Trans. on Power Systems*. Vol. 20, No. 3, August 2005.

[28] J. Usaola, J. Angarita "Bidding wind energy under uncertainty." *Proceedings of the 2007 ICCEP*. Capri (Italy), May 2007.

[29] *Power Systems Test Case Archive*. [Online]. Available: http://www.ee.washington.edu/research/pstca.

[30] Morales J. M., Pérez-Ruiz J., "Point Estimate Schemes to Solve the Probabilistic Power Flow." *IEEE Trans. on Power Systems*. Vol. 22, No. 4, November 2005.